significant difference in the population of binucleated cells compared with control cells (see Supplementary Data, Figure S1). Together, these observations indicate that the overexpression of HCV NS5A is correlated with an increase in the number of cells with mitotic spindles and centrosomes rather than unsuccessful cytokinesis and binucleation.

Next, we compared the expression profiles of mitotic marker proteins, such as phospho-H3, Aurora A, Cyclin A, Cyclin B1, and BubR1, in control Huh7 and Huh7-NS5A cells. Huh7 and Huh7-NS5A cells were cultured in the presence of nocodazole, and cell extracts were prepared at the indicated time-points and resolved by gel electrophoresis at equal loading quantities. Levels of the indicated proteins were assessed by immunoblotting using anti-HA, anti-phospho-H3, anti-Aurora A, anti-Cyclin A, anti-Cyclin B1, anti-BubR1, anti-Cdh1 and anti-Actin antibodies (Figure 4). In control Huh7 cells, phosphorylation of histone H3 was induced at 12 h after nocodazole treatment, peaked at 30 h, and then rapidly decreased (Figure 4(a)), whereas in NS5A-expressing cells, histone H3 phosphorylation was induced at 6 h and maintained for up to 42 h after nocodazole treatment (Figure 4(a)). Because histone H3 phosphorylation occurs during mitosis and is required for proper chromosome condensation and segregation, this result confirms that NS5A protein expression increases the population of cells aberrantly arrested in mitosis. In addition, we examined the expressions of Cyclin A, Cyclin B1, and Aurora A, which play important roles in initiating and maintaining mitotic cell cycle control *via* their specifically timed expressions

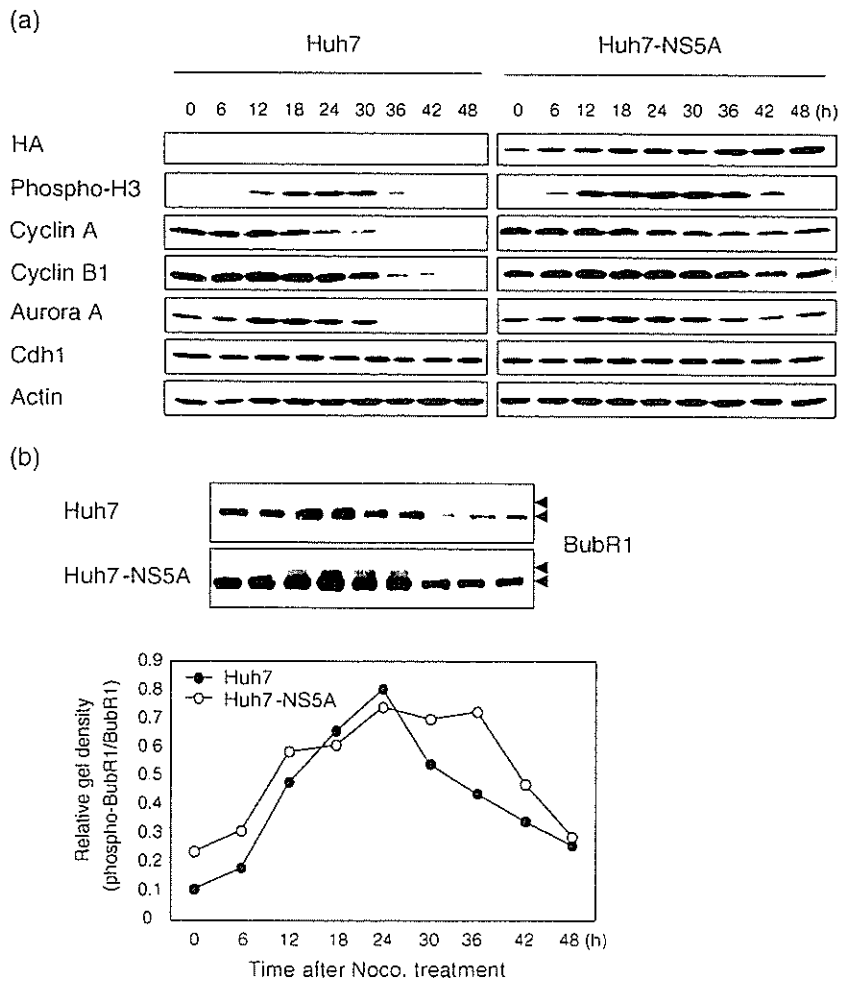

Figure 4. Cells expressing NS5A remained in mitotic arrest for an extended duration. (a) and (b) Huh7 and Huh7-NS5A cells were cultured in the presence of nocodazole (0.1 μg/ml). Cell extracts were prepared at the indicated time-points and were resolved by gel electrophoresis at equal loadings. Levels of the indicated proteins were assessed by immunoblotting using anti-HA, anti-phospho-H3, anti-Aurora A, anti-Cyclin A, anti-Cyclin B1, anti-BubR1, anti-Cdh1, or anti-Actin antibodies. Profiles of BubR1 phosphorylation status in Huh7 and Huh7-NS5A cells are presented as relative gel densities (b). Gel densities of hyperphosphorylated BubR1 (upper arrowhead) and hypophosphorylated BubR1 (lower arrowhead) were quantified by densitometry, and values were obtained by dividing the gel densities of hyperphosphorylated BubR1 by those of hypophosphorylated BubR1.

and degradations (Figure 4(a)). In particular, Cyclin A is destabilized when cells enter mitosis, and is almost completely degraded before the metaphase to anaphase transition.[32–34] Moreover, Cyclin B1 degradation is required for the transition from metaphase into anaphase.[32–34] We found that Cyclin A levels began to decrease 30 h after nocodazole treatment in Huh7 cells, but remained stable for up to 48 h in Huh7-NS5A cells, whereas Cyclin B1 levels decreased at 36 h after nocodazole treatment in Huh7 cells, but accumulated in Huh7-NS5A cells over the entire experimental time course (up to 48 h). On the other hand, Aurora A levels decreased consistently from 36 h after nocodazole treatment in Huh7 cells, but were maintained in Huh7-NS5A cells. Finally, we compared the phosphorylation status of BubR1 protein, because the hyperphosphorylation of BubR1 is known to be a prerequisite of exit from mitotic arrest.[35] In control cells, the hyperphosphorylated form of BubR1 increased from 12 h after nocodazole treatment, peaked at 24 h, and then rapidly decreased (Figure 4(b)). However, in cells expressing NS5A, hyperphosphorylation of BubR1 was detectable from 6 h after treatment and was maintained for up to 42 h (Figure 4(b)). These results collectively indicate that cells expressing NS5A cause aberrant elevations of these mitotic marker proteins and thus perturb the normal timing of the mitotic cell cycle.

Overexpression of HCV NS5A protein induces chromosome aneuploidy

Following prolonged mitotic arrest in response to spindle damage, even cells possessing a competent mitotic checkpoint eventually exit mitosis and undergo apoptosis. However, cells with a persistent mitotic abnormality, such as mutational inactivation of a mitotic checkpoint gene, tend to escape apoptosis and continue cell cycle progression.[21,36–38] Therefore, we questioned whether the aberrant mitotic arrest and mitotic abnormalities induced by NS5A expression could contribute to chromosome missegregation and subsequent aneuploidy. Thus, we treated asynchronized control Huh7 and Huh7-NS5A cells with a microtubule inhibitor (nocodazole) and harvested the cells at various time-points (Figure 5(a)). Interestingly, whereas control Huh7 cells showed marked increases in apoptotic cell populations, Huh7-NS5A cells showed significant increases in aneuploid cells, and these increases were seemingly correlated with duration of exposure to the microtubule inhibitor. In contrast, Huh7-NS5B cells showed reduced apoptosis and increased numbers of cells arrested in the G2/M phases, but no significant accumulation of aneuploid cells (data not shown). To confirm these results, we performed parallel experiments in control Chang-HA and Chang-NS5A cells. As expected, flow cytometric analysis revealed that

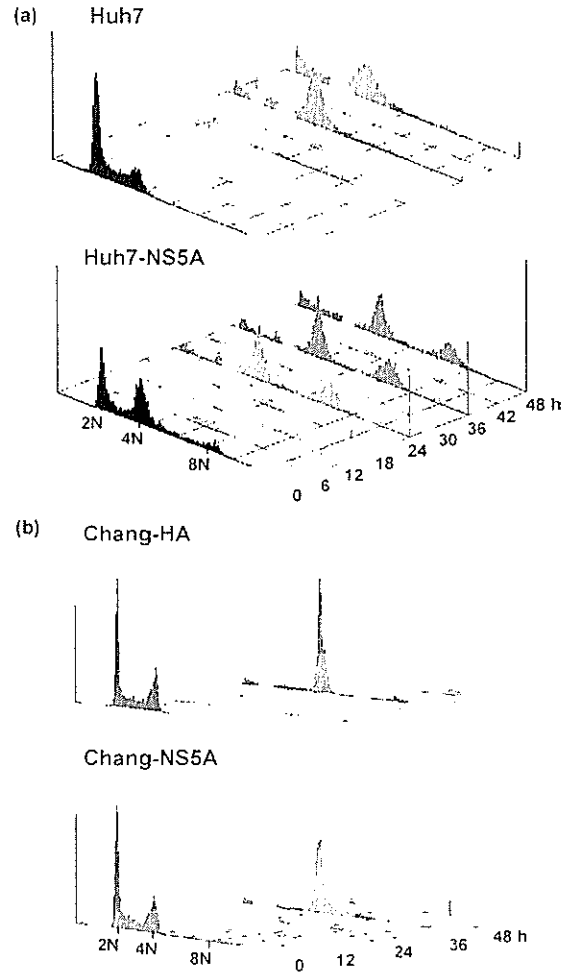

Figure 5. Exogenous expression of HCV NS5A protein induces chromosome aneuploidy. (a) Asynchronized control Huh7 and Huh7-NS5A and (b) Chang-HA and Chang-NS5A cells were treated with nocodazole (0.1 μg/ml). At the indicated time-points, cells were harvested, stained with propidium iodide, and analyzed for DNA content by flow cytometry.

Chang-NS5A cells showed significant accumulations of aneuploid cells compared with control Chang-HA cells (Figure 5(b)). Collectively, our results demonstrate that the expression of HCV NS5A protein induces aneuploidy, and that this appears to be associated with mitotic abnormalities, such as delayed mitotic exit and multi-polar spindle formation.

HCV infection may be directly associated with chromosomal instability

It has been shown that array-based comparative genomic hybridization (CGH) can detect the chromosome aberrations characteristic of human tumors.[39] Here, tumor tissues and adjacent non-tumor tissues were obtained from five HCV-infected patients, all of whom were positive for

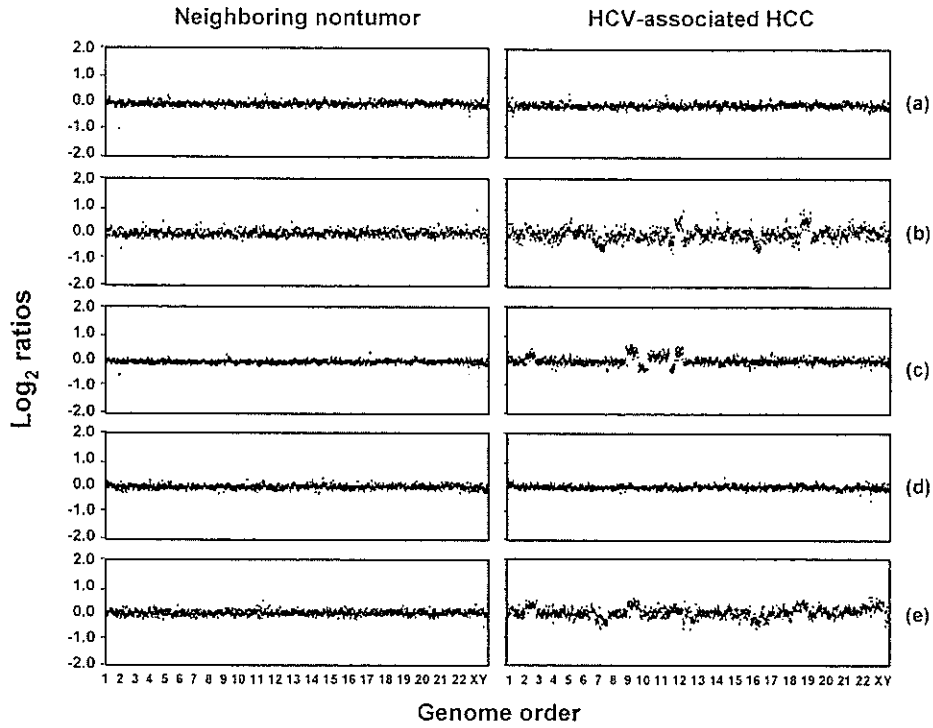

Figure 6. Detection of chromosome aberrations in HCV-associated HCC tumors using CGH arrays. Genomic DNA was isolated from frozen HCV-associated (left panels) and adjacent non-tumor (right panels) tissues from five patients, and subjected to whole genome CGH array analysis with fluorescent *in situ* hybridization (see Materials and Methods). The measured $\log_2$ ratios of the Cy3/Cy5 fluorescence intensities of spots ranged from +0.2 to −0.2. Threshold levels for $\log_2$ ratio gains and losses were set at +0.2 and −0.2, respectively. The *y*-axis indicates the $\log_2$ ratio of quadruplicate measurements per chromosome, and shows chromosome gains or losses. Chromosomes are shown on the *x*-axis, in order from 1p to Xq/Yq. A blinded CGH array study revealed widespread chromosomal aberrations in three of five cases ((b), (c) and (e)).

anti-HCV antibody (HCV-Ab) and HCV RNA, but negative for hepatitis B surface antigen (HBs-Ag). The CGH profiles of these samples are shown in Figure 6. Interestingly, three of the five HCV-associated HCC tumors ((b), (c) and (e)) showed marked chromosome instability, as indicated by widespread chromosome copy number abnormalities. In contrast, no significant indication of widespread genomic alterations was evident in the five adjacent non-tumor tissue samples. Consistent with speculations in previous studies,[16,26,27] these observations provide evidence that HCV infection may be directly associated with chromosomal instability.

Discussion

Here, we provide novel evidence that indicates that cells expressing HCV polyproteins induce chromosomal instability. Furthermore, our findings demonstrate that cells expressing NS5A protein show delayed mitotic exit and mitotic apparatus abnormalities (i.e. multi-polar spindles), which enable cells with unbalanced sets of chromatids segregated at multiple spindle poles to progress to anaphase and telophase. Importantly, we observed similar phenotypes in human primary cells, lung L132 cells, and amniocytes (A139 cell line), by monitoring the ectopic expression of NS5A using a recombinant adenovirus (see Supplementary Data, Figure S2). Thus, repeated failure of balanced chromatids segregation due to persistent HCV protein expression appears to cause widespread chromosome instability and aneuploidy in hepatocytes. During prolonged mitotic arrest, mitotic checkpoint components have been shown to inhibit APC/C, and to prevent it from targeting Cyclin B1 and Securin for degradation.[40] In the present work, we found that NS5A-expressing cells showed increased fractions of mitotic cells and reduced populations of G1 cells, and reduced degradations of APC/C substrates, Cyclin B1 (Figure 4) and Securin (data not shown). These observations indicate that NS5A may be involved in the unscheduled activation of APC/C, and thus, the development of aneuploidy. However, additional study is required to identify the cellular factors targeted by NS5A in this context.

It is widely believed that cells with mitotic abnormalities produce a "wait signal" to delay the onset of anaphase, and that a "fail-safe" mechanism exists to trigger apoptosis in cells that breach the mitotic checkpoint, thus avoiding aneuploidy. However, our results indicate that cells expressing

HCV non-structural proteins somehow adapt to aneuploidy and return to the cell cycle following a sustained mitotic delay. Recent studies have suggested that NS5A exerts an anti-apoptotic effect, and thus confers a viral multiplicative potential in infected cells. In addition, it has been reported that NS5A activates NF-*k*B by inducing oxidative stress in cells.[41] Moreover, liver tissues from chronic hepatitis C patients displayed elevated levels of NF-*k*B[42] and NF-*k*B was shown to induce the expressions of anti-apoptotic factors, such as IAP and Bcl-2.[43] Therefore, it is likely that the persistent expression of NS5A triggers or maintains the expressions of genes that provide protection against apoptotic stimuli, perhaps even during the acute phase of liver disease associated with HCV infection. Consistent with this notion, we observed that cells expressing HCV NS5A and NS5B showed caspase-3 activation inhibition following nocodazole treatment, whereas control cells showed activation of the apoptotic pathway upstream of caspase-9, which sequentially activates caspase-3 (data not shown). Thus, it appears that HCV NS5A interferes with "gatekeeper" cellular functions by blocking apoptotic pathways, thereby enabling cells with mitotic abnormalities and aneuploidy to continue cycling.

HCC tumors are associated with high incidences of genetic alterations, which increase during the carcinogenic process. Moreover, it is known that chronic liver injury caused by HCV infection eventually leads to necrosis, inflammation, and liver regeneration, and that it is frequently associated with an accumulation of genetic alterations, such as, loss of p53 function.[44–46] Cells lacking functional p53 undergo normal mitotic arrest in response to spindle damage, but then subsequently avoid the checkpoint, enter S phase, and endoreduplicate DNA, resulting in aneuploidy.[47] Thus, p53 protein appears to be required to protect normal cells from adaptation to chromosomal instability. In addition, a variety of other genetic and epigenetic aberrations at various stages may collaborate to allow adaptation and aneuploidy. For example, the overexpression of Aurora A (a centrosome-associated serine/threonine kinase) has been implicated in chromosome segregation abnormalities and aneuploidy in many cancer cell types.[48] Smith *et al.*[14] found that Aurora A was upregulated in about 85% of HCV-associated hepatocellular carcinoma tumor samples, and further, the overexpression of Aurora A has been reported to override the mitotic checkpoint and to lead to the premature mitotic exit of cells with inappropriately aligned chromosomes.[49] In the present work, we found that NS5A-expressing cells offered resistance to the normal mitotic cell cycle-dependent destabilization of Aurora A (see Supplementary Data). This suggests that the deregulation of cellular factors, such as Aurora A, acts in concert with HCV non-structural proteins to induce mitotic abnormalities and aneuploidy. However, a previous study provided important evidence that the non-structural proteins of HCV may contribute to hepatic carcinogenesis, whereas structural proteins are a risk factor for the development of steatosis but not liver cancer,[7] which seems to suggest that HCV non-structural proteins are associated with chromosomal instability. In the present study, the frequency and extent of chromosome instability in NS5A-expressing cells was abnormally high even in the absence of a mitotic cell cycle-deregulating stimulus (i.e. nocodazole) (Figure 4), which implies that HCV NS5A protein directly interferes with the normal timing of the mitotic process *in vitro*. However, it should be noted that levels of HCV proteins are very low *in vivo*, i.e. they are not easily detected by routine immunohistochemical assays of HCV-infected liver samples. Thus, NS5A alone may not be sufficient to trigger mitotic abnormalities *in vivo* and other factors may be required to facilitate NS5A-induced aneuploidy. In agreement with a previous report,[29] we also found that NS5B triggers cell cycle arrest in G2, although this aberrant cell cycle arrest was not linked to a mitotic abnormality or chromosomal instability. Thus, our findings suggest that NS5B may help extend the aberrant cell cycle arrest required for adaptation. Moreover, NS5A has been shown to interact functionally with NS5B,[50,51] thus indicating that this non-structural protein may cooperate in HCV-induced mitotic impairments. However, additional work is required to establish a functional link between NS5A and NS5B with respect to hepatocyte mitotic behavior.

The present study demonstrates for the first time that HCV proteins interrupt the normal timing of the mitotic cell cycle and induce the chromosome instability that is frequently observed in malignant tumors. These findings provide important new insights into HCV-associated hepatocarcinogenesis, and may provide a basis for future therapeutic strategies.

Materials and Methods

Generation of cell lines

Human hepatoma-derived cell lines constitutively expressing full-length (Hep394) or fragments of the HCV open reading frame (Hep352 and Hep3294) were generated as described.[28] To generate liver cell lines expressing HA-tagged NS5A and NS5B, HCV genotype 1b cDNAs encoding NS5A and NS5B were inserted into the pCMV-HA vector,[52] and Huh-7 and Chang liver cells were transfected with the constructs or with empty vector (control). Colonies resistant to G418 (GIBCO BRL) were clonally isolated and screened for expression of NS5A or NS5B, using immunoblot and immunofluorescence assays with an anti-HA antibody (Roche).

Chromosome spreading analysis

For cytogenetic analysis of metaphase chromosomes, established cells were incubated with colcemid (0.04 mg/ml) for 4 h, treated with 0.56% (w/v) KCl for 5 min and fixed with methanol/glacial acetic acid (3:1 (v/v)).

Chromosomes were visualized by Giemsa staining and microscopy.

Cell cycle analysis

For flow cytometric analysis of cell cycle profiles, 10^6 cells were plated in 10 cm dishes and cultured in the presence of 0.1 μg/ml nocodazole (Sigma). At the indicated times, cells were harvested, fixed in 70% (v/v) ethanol, washed in phosphate-buffered saline (PBS), and stained with 40 μg/ml propidium iodide (PI) in the presence of 50 μg/ml RNase A for 30 min at room temperature. Samples of 10,000 cells were then analyzed on a Becton Dickinson FACScan flow cytometer (BD Biosciences) and the data were analyzed with the CellQuest software (BD Biosciences). To generate synchronized populations, established clones were arrested at the G1/S boundary by a double thymidine block[34] and then released. At various time-points after release, cells were harvested and analyzed.

For determination of the mitotic index of each population, cells were harvested, resuspended in Cytofix/Cytoperm™ solution (BD Biosciences Pharmingen), washed with Perm/Wash™ buffer (BD Biosciences Pharmingen), and stained with an anti-MPM2 antibody (Dako) in the presence of PI (10 μg/ml final concentration). Samples of 10,000 cells were then subjected to flow cytometric analysis on a FACScan (as above).

Immunoblot analysis

For immunoblot analysis, cells were cultured as described above and then harvested and lysed at the indicated times. Equal amounts of whole cell proteins were resolved by SDS-PAGE, transferred to a nitrocellulose membrane, blocked, and analyzed with anti-phospho-Histone H3 (Upstate Biotechnology), anti-Aurora A (Abcam), anti-Cyclin A (Santa Cruz Biotechnology), anti-Cyclin B1 (Santa Cruz Biotechnology), anti-BubR1 (BD Biosciences Pharmingen), anti-Cdh1 (Oncogene Research Products), or anti-Actin (Sigma) antibodies.

Live cell imaging

To estimate the duration of mitosis, live cells were imaged in ΔT 0.15 mm dishes (IWAKI) in CO_2-independent medium (GIBCO BRL) supplemented with 10% FBS at 37 °C. Every 2 min for 6 h, 0.5 s exposures were acquired using a 20× NA0.75 objective on an LSM 500 META confocal microscope (Carl Zeiss).

Immunofluorescence

Cells were cultured on 18 mm cover-slips, fixed in 5% (v/v) formaldehyde for 10 min, and permeabilized in PBS containing 0.1% Triton X-100 for 5 min. For examination of the sub-cellular localization of HA-tagged NS5A and NS5B, cells were incubated with anti-HA antibody at room temperature for 2 h followed by a further incubation with anti-mouse IgG conjugated with Alexa Fluor 488 (Molecular Probes) for 1 h. To visualize centrosomes and mitotic spindles, cells were incubated with anti-α-tubulin-FITC (Sigma) and anti-γ-tubulin-Cy3 (Sigma) or pericentrin (Abcam) antibodies, respectively, at room temperature for 1 h. Finally, cells were washed, exposed to Hoechst dye for visualization of DNA, and then viewed under an LSM 500 META confocal microscope.

Liver tissue samples and comparative genomic hybridization (CGH)

Surgically dissected materials were collected from patients at the National Cancer Center (NCC), Korea. Informed consent was obtained and specimens were used in accordance with the guidelines of the NCC Tumor Bank Review Committee. Tumor and adjacent non-tumor tissues were sampled from five patients subsequently found to be positive for the anti-HCV antibody (HCV-Ab; LG Biotech) and HCV RNA (Biosewoom), but negative for the hepatitis B surface antigen (HBs-Ag, Bayer).

Tissues were frozen and genomic DNA was isolated with the PUREGENE DNA isolation kit (Gentra). Probes were directly labeled with Cy3-conjugated dUTP and Cy5-conjugated dUTP for the test and reference DNA samples, respectively, using random prime labeling (Invitrogen). Labeled probes were purified and eluted with spin columns (Qiagen), and then hybridized to an array consisting of 1440 BAC clones (350 cancer-related genes and unique STSs with cytological locations confirmed by FISH; GenomArray™, Macrogen†). The hybridization, washing, scanning and analysis were performed according to the GenomArray™ user's manual. Ten simultaneous hybridizations of HCV-associated tumor specimens *versus* the neighboring non-tumor tissues were performed to define the $\log_2$ ratio.

Acknowledgements

We thank members of the laboratory of Chang-Woo Lee for helpful discussions. This work was supported by research grants from the National Cancer Center, Korea and the Korea Health 21 R&D Project, Ministry of Health & Welfare (03-PJ10-PG13-GD01-0002).

Supplementary Data

Supplementary data associated with this article can be found, in the online version, at doi:10.1016/j.jmb.2006.03.020

References

1. Hoofnagle, J. H. (1997). Hepatitis C: the clinical spectrum of disease. *Hepatology*, 26, S15–S20.
2. Llovet, J. M., Burrough, A. & Bruix, J. (2004). Hepatocellular carcinoma. *Lancet*, 362, 1907–1917.
3. Zoulim, F., Chevallier, M., Maynard, M. & Trepo, C. (2003). Clinical consequences of hepatitis C virus infection. *Rev. Med. Virol.* 13, 57–68.
4. Bartenschlager, R. & Lohmann, V. (2000). Replication of hepatitis C virus. *J. Gen. Virol.* 81, 1631–1648.
5. Penin, F., Dubuisson, J., Rey, F. A., Moradpour, D. & Pawlotsky, J. M. (2004). Structural biology of hepatitis C virus. *Hepatology*, 39, 5–19.

† http://bac.macrogen.com

6. Kato, T., Miyamoto, M., Date, T., Yasui, K., Taya, C., Yonekawa, H. *et al.* (2003). Repeated hepatocyte injury promotes hepatic tumorigenesis in hepatitis C virus transgenic mice. *Cancer Sci.* **94**, 679–685.
7. Lerat, H., Honda, M., Beard, M. R., Loesch, K., Sun, J., Yang, Y. *et al.* (2002). Steatosis and liver cancer in transgenic mice expressing the structural and non-structural proteins of hepatitis C virus. *Gastroenterology*, **122**, 352–365.
8. Moriya, K., Fujie, H., Shintani, Y., Yotsuyanagi, H., Tsutsumi, T., Ishibashi, K. *et al.* (1998). The core protein of hepatitis C virus induces hepatocellular carcinoma in transgenic mice. *Nature Med.* **4**, 1065–1067.
9. Moriya, K., Nakagawa, K., Santa, T., Shintani, Y., Fujie, H., Miyoshi, H. *et al.* (2001). Oxidative stress in the absence of inflammation in a mouse model for hepatitis C virus-associated hepatocarcinogenesis. *Cancer Res.* **61**, 4365–4370.
10. Honda, A., Arai, Y., Hirota, N., Sato, T., Ikegaki, J., Koizumi, T. *et al.* (1999). Hepatitis C virus structural proteins induce liver cell injury in transgenic mice. *J. Med. Virol.* **59**, 281–289.
11. Kawamura, T., Furusaka, A., Koziel, M. J., Chung, R. T., Wang, T. C., Schmidt, E. V. & Liang, T. J. (1997). Transgenic expression of hepatitis C virus structural proteins in the mouse. *Hepatology*, **25**, 1014–1021.
12. Matsuda, J., Suzuki, M., Nozaki, C., Shinya, N., Tashiro, K., Mizuno, K. *et al.* (1998). Transgenic mouse expressing a full-length hepatitis C virus cDNA. *Jpn. J. Cancer Res.* **89**, 150–158.
13. Pasquinelli, C., Shoenberger, J. M., Chung, J., Chang, K. M., Guidotti, L. G., Selby, M. *et al.* (1997). Hepatitis C virus core and E2 protein expression in transgenic mice. *Hepatology*, **25**, 719–727.
14. Smith, M. W., Yue, Z. N., Geiss, G. K., Sadovnikova, N. Y., Carter, V. S., Boix, L. *et al.* (2003). Identification of novel tumor markers in hepatitis C virus-associated hepatocellular carcinoma. *Cancer Res.* **63**, 859–864.
15. Attallah, A. M., Tabll, A. A., Salem, S. F., El-Sadany, M., Ibrahim, T. A., Osman, S. & El-Dosoky, I. M. (1999). DNA ploidy of liver biopsies from patients with liver cirrhosis and hepatocellular carcinoma: a flow cytometric analysis. *Cancer Letters*, **142**, 65–69.
16. Kawai, H., Suda, T., Aoyagi, Y., Isokawa, O., Mita, Y., Waguri, N. *et al.* (2000). Quantitative evaluation of genomic instability as a possible predictor for development of hepatocellular carcinoma: comparison of loss of heterozygosity and replication error. *Hepatology*, **31**, 1246–1250.
17. Lengauer, C., Kinzler, K. W. & Vogelstein, B. (1998). Genetic instabilities in human cancers. *Nature*, **396**, 643–649.
18. Pihan, G. & Doxsey, S. J. (2003). Mutations and aneuploidy: co-conspirators in cancer? *Cancer Cell*, **4**, 89–94.
19. Dai, W., Wang, Q., Liu, T., Swamy, M., Fang, Y., Xie, S. *et al.* (2004). Slippage of mitotic arrest and enhanced tumor development in mice with BubR1 haploinsufficiency. *Cancer Res.* **15**, 440–445.
20. Dobles, M., Liberal, V., Scott, M., Benezra, R. & Sorger, P. K. (2000). Chromosome missegregation and apoptosis in mice lacking the mitotic checkpoint protein Mad2. *Cell*, **101**, 635–645.
21. Michel, L., Liberal, V., Chatterjee, A., Kirchwegger, R., Pasche, B., Gerald, W. *et al.* (2001). MAD2 haploinsufficiency causes premature anapahase and chromosome instability in mammalian cells. *Nature*, **409**, 355–359.
22. Shin, H. J., Baek, K. H., Jeon, A. H., Park, M. T., Lee, S. J., Kang, C. M. *et al.* (2003). Dual roles of human BubR1, a mitotic checkpoint kinase, in the monitoring of chromosomal instability. *Cancer Cell*, **4**, 483–497.
23. Jin, D. Y., Spencer, F. & Jeang, K. T. (1998). Human T cell leukemia virus type 1 oncoprotein Tax targets the human mitotic checkpoint protein MAD1. *Cell*, **93**, 81–91.
24. Lavia, P., Mileo, A. M., Giordano, A. & Paggi, M. G. (2003). Emerging roles of DNA tumor viruses in cell proliferation: new insights into genomic instability. *Oncogene*, **22**, 6508–6516.
25. Forgues, M., Difilippantonio, M. J., Linke, S. P., Ried, T., Nagashima, K., Feden, J. *et al.* (2003). Involvement of Crm1 in hepatitis B virus X protein-induced aberrant centriole replication and abnormal mitotic spindles. *Mol. Cell. Biol.* **23**, 5282–5292.
26. Feitelson, M. A., Bun, B., Satiroglu Tufan, N. L., Liu, J., Pan, J. & Lian, Z. (2002). Genetic mechanisms of hepatocarcinogenesis. *Oncogene*, **21**, 2593–2604.
27. Maggioni, M., Coggi, G., Cassani, B., Bianchi, P., Romagnoli, S., Mandelli, A. *et al.* (2000). Molecular changes in hepatocellular dysplastic nodules on microdissected liver biopsies. *Hepatology*, **32**, 942–946.
28. Aizaki, H., Harada, T., Otsuka, M., Seki, N., Matsuda, M., Li, Y. W. *et al.* (2002). Expression profiling of liver cell lines expressing entire or parts of hepatitis C virus open reading frame. *Hepatology*, **36**, 1431–1438.
29. Arima, N., Kao, C. Y., Licht, T., Padmanabhan, R., Sasaguri, Y. & Padmanabhan, R. (2001). Modulation of cell growth by the hepatitis C virus non-structural protein NS5A. *J. Biol. Chem.* **276**, 12675–12684.
30. Meraldi, P., Honda, R. & Nigg, E. A. (2002). Aurora-A overexpression reveals tetraploidization as major route to centrosome amplification in $p53^{-/-}$ cells. *EMBO J.* **21**, 483–492.
31. Fujiwara, T., Bandi, M., Nitta, M., Ivanova, E. V., Bronson, R. T. & Pellman, D. (2005). Cytokinesis failure generating tetraploids promotes tumorigenesis in p53-null cells. *Nature*, **437**, 1043–1047.
32. Gorbsky, G. J. (1997). Cell cycle checkpoints: arresting progress in mitosis. *BioEssays*, **19**, 193–197.
33. den Elzen, N. & Pines, J. (2001). Cyclin A is destroyed in prometaphase and can delay chromosome alignment and anaphase. *J. Cell Biol.* **146**, 1021–1032.
34. Geley, S., Kramer, E., Gieffers, C., Gannon, J., Peters, J. M. & Hunt, T. (2001). Anaphase-promoting complex/cyclosome-dependent proteolysis of human cyclin A starts at the beginning of mitosis and is not subject to the spindle assembly checkpoint. *J. Cell Biol.* **153**, 137–148.
35. Taylor, S. S., Ha, E. & McKeon, F. (1998). The human homologue of Bub3 is required for kinetochore localization of Bub1 and a Mad3/Bub1-related protein kinase. *J. Cell Biol.* **142**, 1–11.
36. Cahill, D. P., Lengauer, C., Yu, J., Riggins, G. J., Willson, J. K., Markowitz, S. D. *et al.* (1998). Mutations of mitotic checkpoint genes in human cancers. *Nature*, **392**, 300–303.
37. Minn, A. J., Boise, L. H. & Thompson, C. B. (1996). Expression of Bcl-xL and loss of p53 can cooperate to overcome a cell cycle checkpoint induced by mitotic spindle damage. *Genes Dev.* **10**, 2621–2631.
38. Taylor, S. S. & McKeon, F. (1997). Kinetochore localization of murine Bub1 is required for normal mitotic timing and checkpoint response to spindle damage. *Cell*, **89**, 727–735.

39. Albertson, D. G. & Pinkel, D. (2003). Genomic microarrays in human genetic disease and cancer. *Hum. Mol. Genet.* **12**, R145–R152.
40. Hwang, L. H., Lau, L. F., Smith, D. L., Mistrot, C. A., Hardwick, K. G., Hwang, E. S. *et al.* (1998). Budding yeast Cdc20: a target of the spindle checkpoint. *Science*, **279**, 1041–1044.
41. Gong, G., Waris, G., Tanveer, R. & Siddiqui, A. (2001). Human hepatitis C virus NS5A protein alters intracellular calcium levels, induces oxidative stress, and activates STAT-3 and NF-kappa B. *Proc. Natl Acad. Sci. USA*, **98**, 9599–9604.
42. Tai, D. I., Tsai, S. L., Chen, Y. M., Chuang, Y. L., Peng, C. Y., Sheen, I. S. *et al.* (2000). Activation of nuclear factor kappaB in hepatitis C virus infection: implications for pathogenesis and hepatocarcinogenesis. *Hepatology*, **31**, 656–664.
43. Mercurio, F. & Manning, A. M. (1999). NF-kappaB as a primary regulator of the stress response. *Oncogene*, **18**, 6163–6171.
44. Hayashi, J., Aoki, H., Arakawa, Y. & Hino, O. (1999). Hepatitis C virus and hepatocarcinogenesis. *Intervirology*, **42**, 205–210.
45. Idilman, R., De Maria, N., Colantoni, A. & Van Thiel, D. H. (1998). Pathogenesis of hepatitis B and C-induced hepatocellular carcinoma. *J. Viral Hepat.* **5**, 285–299.
46. Teramoto, T., Satonaka, K., Kitazawa, S., Fujimori, T., Hayashi, K. & Maeda, S. (1994). p53 gene abnormalities are closely related to hepatoviral infections and occur at a late stage of hepatocarcinogenesis. *Cancer Res.* **54**, 231–235.
47. Andreassen, P. R., Lohez, O. D., Lacroix, F. B. & Margolis, R. L. (2001). Tetraploid state induces p53-dependent arrest of nontransformed mammalian cells in G1. *Mol. Biol. Cell*, **12**, 1315–1328.
48. Zhou, H., Kuang, J., Zhong, L., Kuo, W. L., Gray, J. W., Sahin, A. *et al.* (1998). Tumour amplified kinase STK15/BTAK induces centrosome amplification, aneuploidy and transformation. *Nature Genet.* **20**, 189–193.
49. Jiang, Y., Zhang, Y., Lees, E. & Seghezzi, W. (2003). Aurora A overexpression overrides the mitotic spindle checkpoint triggered by nocodazole, a microtubule destabilizer. *Oncogene*, **22**, 8293–8301.
50. Shimakami, T., Hijikata, M., Luo, H., Ma, Y. Y., Kaneko, S., Shimotohno, K. & Murakami, S. (2004). Effect of interaction between hepatitis C virus NS5A and NS5B on hepatitis C virus RNA replication with the hepatitis C virus replicon. *J. Virol.* **78**, 2738–2748.
51. Shirota, Y., Luo, H., Qin, W., Kaneko, S., Yamashita, T., Kobayashi, K. & Murakami, S. (2002). Hepatitis C virus (HCV) NS5A binds RNA-dependent RNA polymerase (RdRP) NS5B and modulates RNA-dependent RNA polymerase activity. *J. Biol. Chem.* **277**, 11149–11155.
52. Lee, C. W., Sorensen, T. S., Shikama, N. & La Thangue, N. B. (1998). Functional interplay between p53 and E2F through co-activator p300. *Oncogene*, **16**, 2695–2710.

Edited by J. Karn

(Received 17 October 2005; received in revised form 3 March 2006; accepted 9 March 2006)
Available online 29 March 2006

Available online at www.sciencedirect.com
SCIENCE DIRECT®
Virology 351 (2006) 381–392
VIROLOGY
www.elsevier.com/locate/yviro

Production of infectious hepatitis C virus particles in three-dimensional cultures of the cell line carrying the genome-length dicistronic viral RNA of genotype 1b

Kyoko Murakami [a], Koji Ishii [a], Yousuke Ishihara [b], Sayaka Yoshizaki [a], Keiko Tanaka [c], Yasufumi Gotoh [d,e], Hideki Aizaki [a], Michinori Kohara [f], Hiroshi Yoshioka [g], Yuichi Mori [g], Noboru Manabe [d], Ikuo Shoji [a], Tetsutaro Sata [c], Ralf Bartenschlager [h], Yoshiharu Matsuura [i], Tatsuo Miyamura [a], Tetsuro Suzuki [a,*]

[a] *Department of Virology II, National Institute of Infectious Diseases, 1-23-1 Toyama, Shinjuku-ku, Tokyo 162-8640, Japan*
[b] *Hamaichi Ultrastructure Research Institute, Okazaki, Aichi 444-0076, Japan*
[c] *Department of Pathology, National Institute of Infectious Diseases, Shinjuku, Tokyo 162-8640, Japan*
[d] *Research Unit for Animal Life Sciences, Animal Resource Science Center, The University of Tokyo, Iwama, Ibaraki 319-0206, Japan*
[e] *Unit of Anatomy and Cell Biology, Department of Animal Sciences, Kyoto University, Kyoto 606-8502, Japan*
[f] *Department of Microbiology and Cell Biology, Tokyo Metropolitan Institute of Medical Science, Bunkyo-ku, Tokyo 113-8613, Japan*
[g] *Mebiol Inc., Hiratsuka, Kanagawa 254-0075, Japan*
[h] *Department of Molecular Virology, Hygiene Institute, University Heidelberg, Im Neuenheimer Feld 345, D-69120 Heidelberg, Germany*
[i] *Department of Molecular Virology, Research Institute for Microbial Diseases, Osaka University, Suita, Osaka 565-0871, Japan*

Received 5 January 2006; returned to author with revision 23 January 2006; accepted 24 March 2006
Available online 6 May 2006

Abstract

We show that a dicistronic hepatitis C virus (HCV) genome of genotype 1b supports the production and secretion of infectious HCV particles in two independent three-dimensional (3D) culture systems, the radial-flow bioreactor and the thermoreversible gelation polymer (TGP), but not in monolayer cultures. Immunoreactive enveloped particles, which are 50–60 nm in diameter and are surrounded by membrane-like structures, are observed in the culture medium as well as at the endoplasmic reticulum membranes and in dilated cytoplasmic cisternae in spheroids of Huh-7 cells. Infection of HCV particles is neutralized by anti-E2 antibody or patient sera that interfere with E2 binding to human cells. Finally, the utility of the 3D-TGP culture system for the evaluation of antiviral drugs is shown. We conclude that the replicon-based 3D culture system allows the production of infectious HCV particles. This system is a valuable tool in studies of HCV morphogenesis in a natural host cell environment.

Keywords. Hepatitis C virus; Replication; Three-dimensional culture; Virus particle

Introduction

Infection with hepatitis C virus (HCV) currently represents a major medical and socioeconomic problem. HCV is a main causative agent of chronic hepatitis, cirrhosis, and hepatocellular carcinoma, and there are an estimated 170 million HCV carriers worldwide (Choo et 98). The standard treatments for HCV infection are interferon alpha (IFN-α) in combination with ribavirin (RBV) or, more recently, a polyethylene glycol-modified form of IFN-α; however, sustained response is seen in only ~50% of treated patients (Di et Mi se 00). Further development of new anti-HCV drugs and vaccines has been obstructed by the lack of either a small animal model or a robust cell culture system capable of supporting viral replication and the production of infectious progeny.

HCV is a small enveloped RNA virus belonging to the family Flaviviridae and harboring a single-stranded RNA genome with

* Corresponding author. Fax: +81 3 5285 1161
E-mail address: tesuzuki@nih.go.jp (T. Suzuki).

0042-6822/$ - see front matter © 2006 Elsevier Inc. All rights reserved.
doi:10 016 virol.2006 03 038

positive polarity. A precursor polyprotein of ~3000 amino acids (aa) is encoded by a large open reading frame. This polyprotein is cleaved by cellular and viral proteases to give rise to a series of structural and nonstructural proteins (Choo et al., 1991; Grakoui et al., 1993; Hijikata et al., 1991). The establishment of selectable dicistronic HCV RNAs that are capable of autonomous replication in human hepatoma Huh-7 cells was a significant breakthrough in HCV research (Blight et al., 2000; Lohmann et al., 1999) and has provided an important tool for the study of HCV replication mechanisms and for screening antiviral drugs (Frese et al., 2001, Guo et al., 2001). This replicon system was first developed to replicate only viral subgenomic RNAs but has been further expanded to enable the replication of genome-length dicistronic RNAs (Ikeda et al., 2002; Pietschmann et al., 2002). Although the viral genome replicates and all HCV proteins are properly processed in this system, virus particle production has not yet been achieved. A number of researchers (Date et al., 2004; Kato et al., 2001, 2003) have developed an HCV genotype 2a replicon (JFH-1) that efficiently replicates in a variety of human cells. Recently, it has been demonstrated that the full-length JFH-1 genome or a chimeric genome using JFH-1 and J6, a related genotype 2a strain, produces infectious particles in cell cultures (Lindenbach et al., 2005; Wakita et al., 2005; Zhong et al., 2005). More recently, production of infectious genotype 1a virus (Hutchinson strain) using similar experimental systems has been described (Yi et al., 2006). These complete HCV culture systems produce robust levels of infectious virus and provides a powerful tool for HCV research. However, to date their applications have not been extended to constructs based on strains of genotype 1b, which is highly prevalent worldwide.

We previously demonstrated that differentiated human hepatoma FLC4 cells transfected with in vitro transcribed HCV genomic RNA can produce and secrete infectious particles in three-dimensional (3D) radial-flow bioreactor (RFB) culture (Aizaki et al., 2003). This RFB system was initially aimed to develop artificial liver tissue, and the bioreactor column consists of a vertically extended cylindrical matrix through which liquid medium flows continuously from the periphery toward the center of the reactor (Kawada et al., 1998). In RFB culture, human hepatocellular carcinoma-derived cells can grow spherically or cubically, and they retain liver functions such as albumin synthesis (Kawada et al., 1998; Matsuura et al., 1998) and drug-metabolizing activity mediated by cytochrome P450 3A4 (Iwahori et al., 2003).

In the present study, two kinds of 3D culture techniques, the RFB and the thermoreversible gelation polymer (TGP), were used for the production and secretion of infectious HCV particles by using a dicistronic HCV genome derived from genotype 1b. We also demonstrate that these 3D culture systems are useful for evaluating anti-HCV drugs.

Results

Secretion of HCV-LPs from RCYM1 carrying genome-length dicistronic HCV RNA cultured in RFB culture

We first assessed the replicative capacity of selectable genome-length HCV RNAs in FLC4 cells. However, no G418-resistant colonies were observed, indicating that FLC4 cells do not support replication of these HCV RNAs (data not shown). Therefore, subsequent experiments were carried out with a stable Huh-7 cell line, RCYM1, which supports full-length HCV RNA replication and which was developed by transfection of the cells with genome-length dicistronic RNA derived from the Con1 clone 1389neo/core-3′/NK 5.1 (genotype 1b)

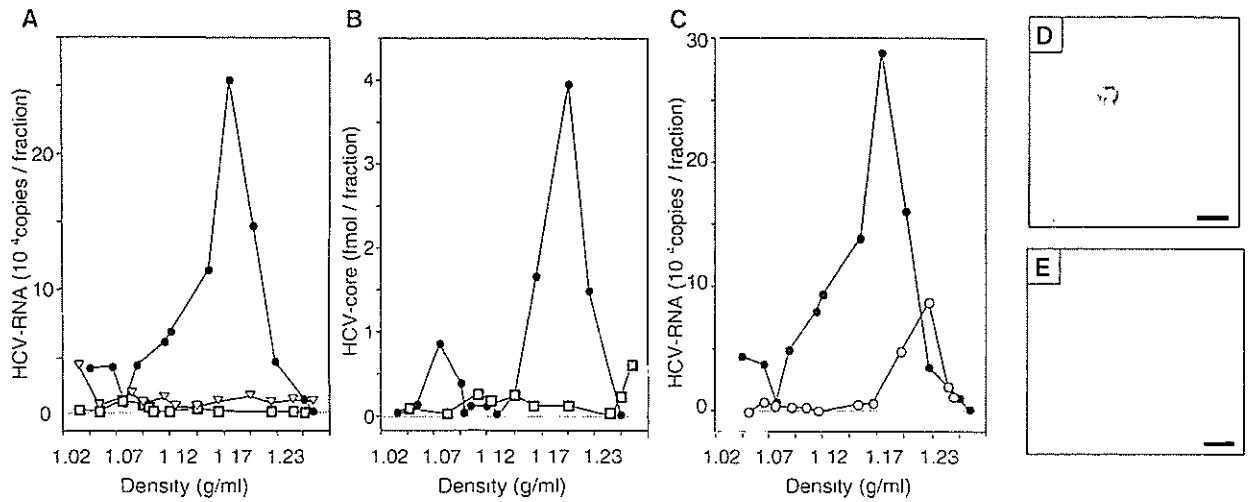

Fig. 1 Sucrose density gradient analysis of culture supernatants of RCYM1 cells. Culture media collected from radial-flow bioreactor (RFB)-cultured RCYM1 (closed circles), monolayer-cultured RCYM1 (open squares), and RFB-cultured 5–15 cells (open triangles) were fractionated as described in Materials and methods. (A) HCV RNA in each fraction was measured by real-time reverse transcriptase-polymerase chain reaction (RT-PCR). Mean values of duplicates were plotted against the density of the corresponding fraction. (B) HCV core protein in each fraction was determined by enzyme-linked immunosorbent assay (ELISA). Mean values of duplicates were plotted against the density. (C) Culture medium of RFB-cultured RCM1 cells were treated with 0.2% NP40 (open circles), followed by centrifugation in a sucrose gradient. Each fraction was tested for HCV RNA by real-time RT-PCR. (D, E) Electron microscopy analysis. Samples were prepared from the 1.18 g/ml fraction of culture media collected from RFB-cultured (D) or monolayer-cultured (E) RCYM1 cells.

(Pietschmann et al., 2002). The HCV RNA level in RCYM1 cells was approximately 5×10^6 copies/μg total RNA as determined by real-time reverse transcriptase-polymerase chain reaction (RT-PCR). The expression and subcellular localization of HCV protein were confirmed by Western blotting and immunofluorescence analysis (data not shown). To develop 3D RFB cultures, first we loaded RCYM1 cells onto an RFB column by flowing cell suspension, after which the cells were attached to carrier beads. Cells proliferated within the 3D matrix, and culture medium was circulated radially through the column.

In order to investigate whether HCV-like particles (HCV-LPs) were secreted from RCYM1 cells in the RFB culture system, we fractionated culture fluid collected after 5–10 days of culture by continuous 10–60% (wt/vol) sucrose density gradient centrifugation. HCV RNA and core protein were predominantly detected in the 1.15–1.20 g/ml fractions, with maximal detection in the 1.18 g/ml fraction (Figs. 1A and B). In the same experiment using 5–15 cells, in which a subgenomic HCV replicon replicates, no peak similar to that observed in RCYM1 cells corresponding to HCV RNA was detected. In both RCYM1 cells and 5–15 cells in the RFB culture system, a substantial amount of HCV RNA was detected in the 1.03–1.07 g/ml fractions (Fig. 1A). Consistent with a previous report by Pietschmann et al. (2002), these RNAs released from cells with a subgenomic replicon did not correspond to virus particles. When an equivalent number of RCYM1 cells were cultured in a monolayer culture system, limited amounts of HCV RNA and core protein were detected in the culture supernatant (Figs. 1A and B).

The mature HCV virion is thought to have a nucleocapsid and an outer envelope composed of a lipid membrane with viral envelope glycoproteins. Culture fluids were treated with NP40 in order to solubilize lipids and were then subjected to sucrose density gradient centrifugation. HCV RNA sedimented to a density of 1.22 g/ml rather than 1.18 g/ml (Fig. 1C), indicating that the density of HCV particles became higher due to de-envelopment. Transmission electron microscopy (TEM) of the 1.18 g/ml fraction, which was subjected to negative staining after concentration, revealed particle structures with diameters of 30–60 nm and a major particle size of 50 nm (Fig. 1D). No similar particle-like structures were observed in the same density fraction of the RCYM1 monolayer culture (Fig. 1E) or in the 1.23 g/ml fraction of the RCYM1-RFB culture (data not shown). These results indicate that, in the RFB system, the production and secretion of HCV-LPs is possible with a selectable dicistronic HCV genome.

Production and secretion of HCV-LPs from spheroid culture of RCYM1 cells using TGP

In the 3D RFB culture system for RCYM1 cells, extracellular secretion of HCV-LPs was observed. Based on this observation, we hypothesized that morphological changes occurring in 3D culture, such as polarity formation, promote advantageous in the assembly of viral proteins, particle formation, and extracellular secretion. To examine whether similar phenomena could be observed in other 3D culture systems, we investigated HCV-LP expression using a 3D culture system with TGP as a carrier.

TGP is a biocompatible polymer made from conjugates of polyethyleneglycol and poly-*N*-isopropylacrylamide, which is a thermoresponsive polymer composed of *N*-isopropylacrylamide and *n*-butylmethacrylate. The TGP solution possesses sol-gel transition properties; it is water soluble (sol phase) at temperatures below the transition temperature, and it is insoluble (gel phase) above it. It is possible to manipulate the transition temperatures through molecular engineering. The transition temperature for TGP in the present experiments was approximately 20 °C.

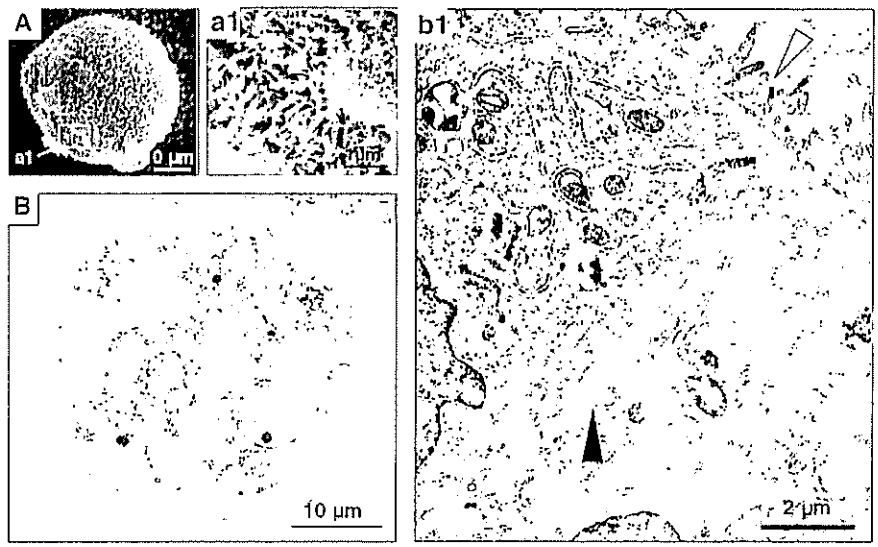

Fig. 2. Huh-7 and RCYM1 cells form spheroids in thermoreversible gelation polymer (TGP). Scanning electron microscopy (A and a1) and transmission electron microscopy (B and b1) of RCYM1 cells cultured in TGP for 8 days. Open arrowhead, microvilli; closed arrowheads, bile canaliculi-like structures.

RCYM1 cells, which were seeded into the TGP, formed three-dimensional compacted aggregates called spheroids after 3 days of culture, and numerous spheroids with diameters of approximately 1 mm were observed after 7–10 days of culture. After 8 days of culture, the spheroids were fixed and examined by scanning electron microscopy (Figs. 2A and a1) and ultrathin sections were examined by TEM (Figs. 2B and b1). Well-developed microvilli, a feature of polarized epithelium, were observed on the cell surface (Figs. 2A and a1). Bile canaliculi-like structures were also observed within intercellular spaces, and they appeared to be connected via tight junctions (Figs. 2B and b1). This cytomorphology, similar to that observed in the RFB culture (Kawada et al., 1998; Matsuura et al., 1998), correlated well with the features of mature liver tissue.

It is known that the replication of HCV replicons in Huh-7 cells depends on host cell growth. We found that the growth of RCYM1 cells in the TGP culture system was significantly slower than that of cells in monolayer culture (Fig. 3A). Accordingly, the expression of HCV proteins (Fig. 3B) in the RCYM1 spheroids was apparently lower compared to those observed in the monolayer cells. The viral RNA copy number in the spheroids was approximately one tenth of that in the monolayer culture (data not shown). The results of sucrose density gradient analysis of culture supernatant demonstrated co-sedimentation of HCV RNAs and core proteins at a density of 1.15–1.20 g/ml, with a peak at 1.18 g/ml (Figs. 3C and D). This distribution was consistent with the pattern obtained in RFB culture (Figs. 1A and B). It should be noted that in these experiments, lower cell numbers were used in the 3D cultures than in the monolayer cultures because of the slower growth of cells. As estimated from the quantitative data of the 1.15–1.20 g/ml fractions of the culture supernatants, 0.1–1 copies of HCV RNA/cell/day are produced and assembled into viral particles in the TGP-cultured RCYM1 cells.

TEM analysis of the 1.18 g/ml fraction after negative staining showed particle structures with a diameter of 50–60 nm and spike-like projections (Fig. 3E). Observation of ultrathin sections indicated a lipid bilayer-like membrane structure with a

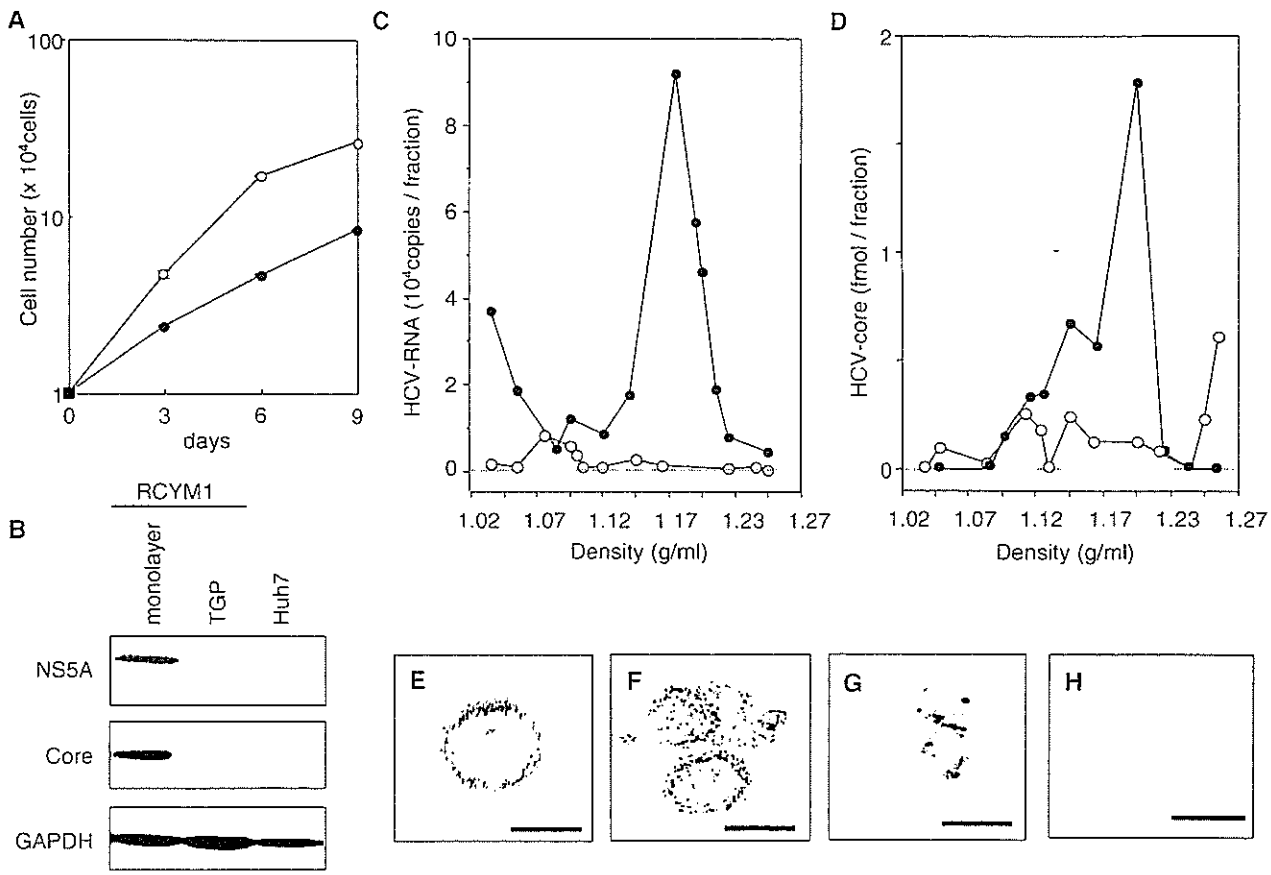

Fig. 3. Expression of HCV proteins in RCYM1 cells and secretion of viral particles in TGP culture. (A) Cell growth curves of the TGP (closed circles) and monolayer (open circles) culture of RCYM1 cells. Cells were harvested at days 0, 3, 6, and 9 postinoculation and cell numbers were determined. (B) Western blotting of HCV core and NS5A proteins in RCYM1 cells and control Huh-7 cells. (C, D) Sucrose density gradient analysis of culture supernatants of RCYM1 cells. The culture supernatants were fractionated as described in Materials and methods. HCV RNA (C) and core protein (D) in each fraction were determined by ELISA and real-time RT-PCR, respectively. Representative data from three independent experiments are shown. Closed circles, TGP culture; open circles, monolayer culture. (E–H) Electron microscopy of HCV-like particles (HCV-LPs) in the supernatants of TGP-cultured RCYM1 cells. (E) Negative staining of HCV-LPs in the 1.18 g/ml density fraction. There was no spherical structure in 1.05 g/ml density fraction, as shown in panel H. (F) Ultrathin section of HCV-LPs. Precipitated HCV-LP samples were prepared from the 1.18 g/ml fraction as described in Materials and methods. (G) Immunogold labeling of HCV-LPs with an anti-E2 antibody in the 1.18 g/ml density fraction. Gold particles, 5 nm; scale bars, 50 nm.

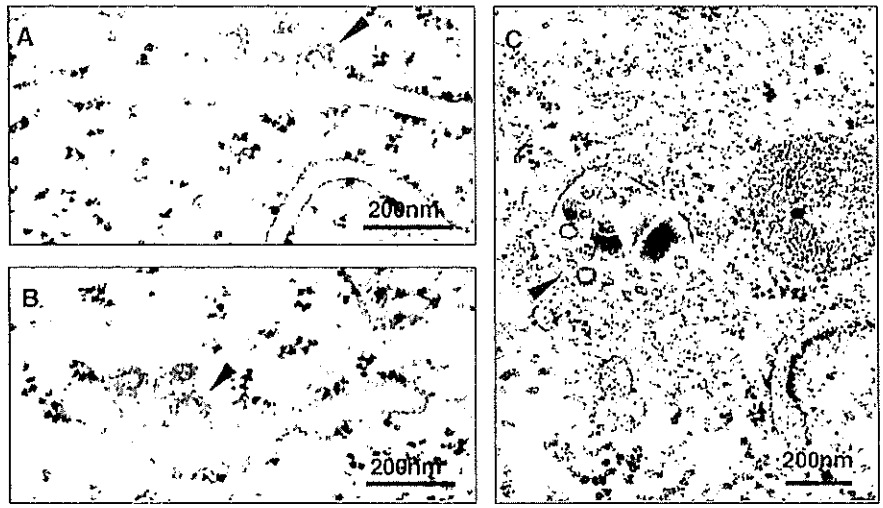

Fig. 4. Electron microscopy of ultrathin sections of RCYM1 cells grown in TGP. HCV-LPs in TGP-cultured RCYM1 cells. Spherical virus-like particles 50–60 nm in diameter (arrowheads) were observed at the ER membranes (A, B) and in the cytoplasmic vesicles (C).

width of approximately 5 nm (Fig. 3F). Immunoelectron microscopic study using anti-E2 antibody revealed HCV envelope protein(s) on the particle surface (Fig. 3G). Substantial amounts of HCV RNA were detected in the 1.03–1.05 g/ml fractions of the supernatant (Fig. 3C); however, HCV-LP structures were not observed in these fractions (Fig. 3H). These results were consistent with those from the RFB system, as shown above. The efficacy of 3D cell culture systems in virion formation was thus demonstrated in both the RFB and TGP culture systems using human liver-derived cells.

Ultrastructural localization of HCV-LPs in TGP-cultured spheroids of RCYM1 cells

We next determined the intracellular localization of HCV-LPs produced in RCYM1-TGP culture at the ultrastructural level by electron microscopic (EM) analysis of ultrathin sections. Spherical particles having membrane-like structures with short surface projections (diameter, 50–60 nm) were observed primarily at the endoplasmic reticulum (ER) membrane (Fig. 4A) as well as in the dilated cisternae of the ER (Fig. 4B). In vesicles, these virus-like particles were frequently associated with amorphous materials (Fig. 4C). In a previous study, Shimizu et al. (1996) report that virus-like particles with similar morphology and size were observed in human B cells infected with HCV. No similar particle-like structures were observed in RCYM1 cells in monolayer culture or in subgenomic replicon 5–15 in cells in TGP culture (data not shown).

In order to determine whether the virus-like particles observed by conventional TEM in the present experiment were HCV-LPs, we conducted immunoelectron microscopic analysis with anti-core antibody and anti-E1 antibody. Double-labeling experiments showed that the virus-like particles associated with the ER membrane exhibited immunoreactivity for both HCV proteins, and that the E1 protein surrounded the core proteins (Fig. 5A). To the best of our knowledge, this is the first report to clearly demonstrate that the viral envelope protein surrounds the core protein in HCV particle formation. As a negative control, thin sections prepared from subgenomic RNA containing 5–15 cells were stained with these antibodies and were found to exhibit negligible levels of background immunostaining (data not shown).

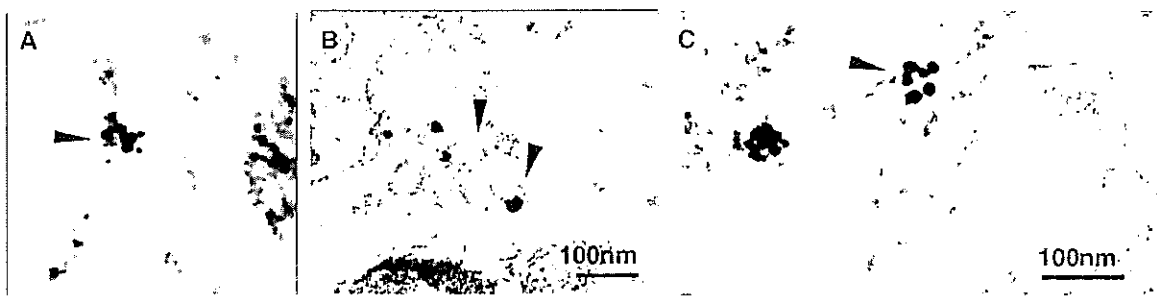

Fig. 5. Immunoelectron microscopy of ultrathin sections of TGP-cultured RCYM1 cells. (A) Double immunostaining with anti-E1 and anti-core monoclonal antibodies. Core protein-specific gold particles (10 nm in diameter) and E1 protein-specific gold particles (5 nm in diameter) formed rosettes on the surface of the ER membrane. (B and C) Silver-intensified immunogold staining with anti-core (B) and anti-E1 (C) antibodies. The second antibody conjugated with gold particles 1.4 nm in diameter was applied, followed by enlargement of the particles by the silver enhancement reagent. Arrowheads indicate virus-like particles reacting with anti-core and/or anti-E1 antibodies.

It is generally difficult to visualize intracellular microstructures and perform antigenic protein localizations using immunogold electron microscopy due to the low resolution and contrast of micrographs. In order to overcome this difficulty, we applied a silver-intensified immunogold labeling method in our experiment (Figs. 5B and C). Using this method, antigen-reactive immunogold particles approximately 20 nm in diameter were observed. Specific immunolabeling of core and E1 protein was detected in the ER or on the ER membranes. Intense immunopositive reactions were also seen on the virus-like particles observed in cytoplasmic vesicles and on ER membranes; however, no such immunolabeling was observed when normal mouse serum was used as a first antibody (data not shown). These results confirm the ultrastructural observations of conventional TEM and suggest that the formation of HCV particles is achieved by budding of the putative core particles at the ER membrane.

Infectivity of HCV-LPs depends on E2 glycoprotein

To determine whether HCV-LPs released from RCYM1 cells cultured in the TGP system are infectious, we inoculated naive Huh-7.5.1 cells (Zhong et al., 2005), which are HCV-negative Huh-7.5 (Blight et al., 2002)-derived cells, with a culture supernatant of RCYM1 spheroids. HCV RNAs in the cells at days 0, 1, 2, 3, and 7 postinoculation were determined by real-time RT-PCR. Fig. 6A shows the kinetics of HCV RNA after the inoculation of HCV-LPs. HCV RNA levels in the infected Huh-7.5.1 cells fluctuated at the indicated times, reaching 10^3–10^4 copies/μg of cellular RNA at days 1–7. Immunofluorescence staining 4 days postinoculation revealed that approximately 1% of cells were positive for NS5A protein (Fig. 6B). In contrast, no NS5A-positive cells were detected when the cell supernatant sample obtained from 5 to 15 cell cultured in TGP was used to inoculate Huh-7.5.1 cells (data not shown). These results suggest that HCV-LPs released from TGP-cultured RCYM1 cells are infectious.

To further determine whether viral envelope proteins mediate infection by HCV-LPs, we preincubated HCV-LPs with the anti-E2 monoclonal antibody AP33, which demonstrates potent neutralization of infectivity against HCV pseudoparticles carrying E1 and E2 proteins representative of the major genotypes 1 through 6 (Owsianka et al., 2005), or with patient sera with high titers of HCV neutralization of binding (NOB) antibodies (Ishii et al., 1998), or with anti-FLAG antibody (Fig. 6C). NOB antibodies have the ability to neutralize the binding of E2 protein to human cells (Rosa et al., 1996), and NOB3 and NOB4 were sera obtained from patients who recovered naturally from chronic hepatitis C (Ishii et al., 1998). Intracellular HCV RNA levels were decreased by 43%, 28%,

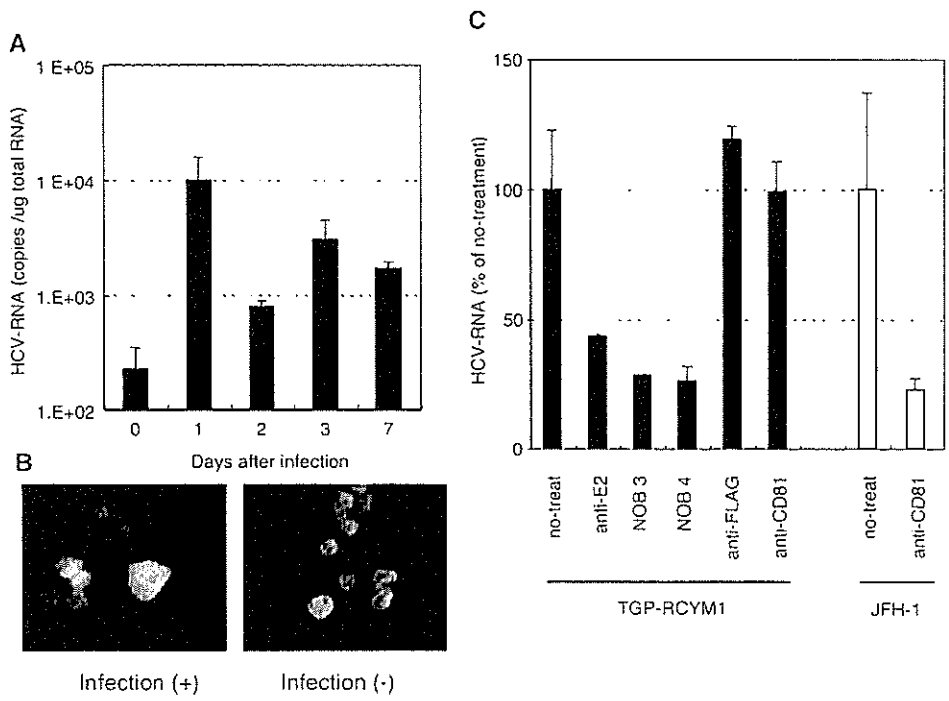

Fig. 6. Infectivity of HCV-LPs secreted from TGP-cultured RCYM1 cells and neutralization of the infection. (A) Kinetics of HCV RNA after the infection of HCV-LPs. Huh-7.5.1 cells were infected with HCV-LPs and harvested at days 0, 1, 2, 3, and 7. HCV RNAs in the cells were determined by real-time RT-PCR. (B) Huh-7.5.1 cells infected with HCV-LPs (upper panel) or without infection (lower panel) were cultured for 4 days, followed by immunostaining with anti-NS5A antibody. Nuclei were counterstained with 4′,6-diamidino-2-phenylindole (DAPI). (C) Huh-7.5.1 cells were infected with HCV-LPs after pretreatment with anti-E2 antibody AP33, neutralization of binding (NOB) antibodies, or anti-FLAG antibody. Anti-human CD81 antibody was preincubated with Huh-7.5.1 cells prior to the infection. Huh-7.5.1 cells were infected with HCV-LPs derived from TGP-cultured RCYM1 cells or JFH1 virus and incubated for 4 days: HCV RNAs in the cells were determined by real-time RT-PCR. The inhibition rate is given as the percentage of the no-treatment controls. Average values with standard deviations in triplicate samples are shown. Closed bars, HCV-LPs secreted from TGP-cultured RCYM1 cells; shaded bars, JFH1 virus.

and 26% in the presence of AP33, NOB3, and NOB4, respectively. No reduction of viral RNA in infected cells was observed following treatment with anti-FLAG antibody. Thus, the present results suggest that viral envelope proteins play a crucial role in the infectivity of HCV-LPs produced by RCYM1 cells cultured in TGP. We further tested anti-CD81 antibody for inhibition of the virus infection in our system. As shown in Fig. 6C, pretreatment of the cells with the anti-CD81 antibody resulted in no inhibition of the intracellular HCV RNA level in the infected cells. In contrast, under the same condition of treatment, the antibody efficiently inhibited the infection of JFH-1 virus, which was produced from the HCV JFH-1 molecular clone as previously described (Wakita et al., 2005; Zhong et al., 2005), suggesting that CD81 has no or little, if any, need for the infection of HCV produced in our system.

Potential use of the TGP culture system for HCV production and evaluation of antiviral agents

In a recent report, Lindenbach et al. (2005) found that a cell culture system supporting complete replication of an HCV genotype 2a clone is useful for the evaluation of antiviral drugs. However, to date this complete HCV culture system has not been extended to genotype 1b, which is more frequently detected in patients with hepatitis C and is the most difficult to treat.

We show here the potential utility of the TGP culture of RCYM1 cells for evaluating anti-HCV drugs (Fig. 7). Intracellular HCV RNA levels in TGP-cultured RCYM1 cell spheroids were reduced by 90% after 3 days of culture with 100 IU/ml of IFN-α (Fig. 7A). Likewise, the extracellular HCV particle level, which was calculated using the HCV RNA copy number of the 1.18 g/ml supernatant fraction, was reduced by 89% by IFN-α treatment (Fig. 7B). Moreover, the production of HCV particles was inhibited by treatment with 100 μM RBV to the same degree (85%) as intracellular HCV RNA (Fig. 7B). The level of HCV RNA detected in the 1.04 g/ml fraction of the culture supernatant of the untreated group was approximately one fourteenth of that in the 1.18 g/ml fraction, and the level increased with the addition of IFN-α or RBV (Fig. 7B). Although the mechanism underlying this increase is unknown, a similar phenomenon was observed when several highly cytotoxic agents were evaluated using TGP-RCYM1 cultures (data not shown). It is therefore likely that some cellular proteins associated with HCV RNA are released into the culture supernatant as a result of cell death caused by the moderate cytotoxic effects of IFN and RBV.

Collectively, these results demonstrate that the HCV production model based on TGP culture is useful for evaluating HCV particle production and the inhibitory effects of anti-HCV drugs.

Discussion

In the present report, we describe that HCV-LPs are assembled and released from Huh-7 cells harboring a dicistronic genome-length Con1 HCV RNA in two independent 3D culture systems. The HCV-LPs closely resemble virus-like particles detected in the sera of patients with hepatitis C in terms of both particle size and morphology. The HCV-LPs released into the culture supernatant have a buoyant density of approximately 1.18 g/ml, which is much higher than that of putative HCV particles isolated from patient sera reported previously (Andre et al., 2002, Kanto et al., 1994; Nakajima et al., 1996; Trestard et al., 1998) and slightly higher than the average density of virus particles produced with the JFH-1 isolate (Wakita et al., 2005). One possible explanation is that the HCV particles are highly bound to lipids and low-density lipoproteins in patient sera. In agreement with a recent report (Wakita et al., 2005), our EM examination demonstrated that HCV-LPs are 50–60 nm in diameter and are composed of core-like particles with a diameter of approximately 30 nm that are surrounded by ER-derived E1/

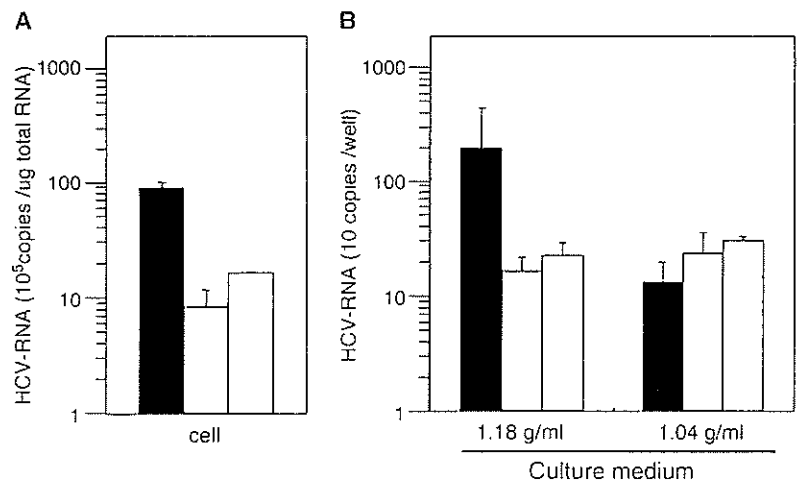

Fig. 7. Inhibition of HCV-LP production by IFN and RBV. TGP-cultured RCYM1 cells were treated with 100 IU/ml IFN-α or 100 μM RBV, and HCV RNAs in the cells (A) and in the culture media (B) were then determined. Culture media from each sample were fractionated by sucrose gradient centrifugation and HCV-LP positive (1.18 g/ml) and negative (1.04 g/ml) fractions were assayed. Average values with standard deviations in triplicate samples are shown. Closed bars, no-treatment control; shaded bars, IFN-α; open bars, RBV.

E2 proteins. These particles are observed at the ER membranes and in dilated cisternae of the ER, suggesting that the interaction of the ER membrane containing HCV envelope proteins with the viral core protein drives the budding process of HCV particles into the ER lumen.

Although studies on the ultrastructure and morphogenesis of HCV-LPs have been conducted using recombinant viral vectors carrying HCV structural protein genes (Baumert et al., 1998; Blanchard et al., 2002, 2003), the present study provides the first visual evidence of assembly and budding of HCV particles in a heterologous expression system in which a full-length viral genome is replicating and the viral particles are secreted into the culture medium. We also demonstrated that the HCV-LPs produced in our 3D culture system are infectious and that their infection is prevented by the monoclonal antibody AP33 directed against E2 (Owsianka et al., 2005) as well as by NOB antibodies (Ishii et al., 1998), which are sera of patients naturally resolving from chronic hepatitis C and exhibiting neutralizing activity. This result is consistent with the recent demonstration that E2 is required for the infectivity of JFH-1 virus (Wakita et al., 2005). It has been shown that CD81 interacts with E2 (Pileri et al., 1998) and that anti-CD81 antibodies or a soluble CD81 fragment block the infection of Huh-7 cells with either pseudotyped retroviral particles, JFH-1 virus or J6/JFH1 chimera (Lindenbach et al., 2005; Netski et al., 2005; Wakita et al., 2005; Zhong et al., 2005). Inconsistent with these studies, however, we found that anti-CD81 antibody did not inhibit the virus infection in our system. Although CD81 is considered to represent an important component in HCV entry, there are several other candidate cellular receptors for HCV (Bartosch and Cosset, 2006) and a study has demonstrated that in vitro binding of HCV to hepatoma cell lines was not inhibited by the anti-CD81 antibody (Sasaki et al., 2003).

In a previous report (Aizaki et al., 2003), we describe the production and release of infectious HCV particles from a human hepatocellular carcinoma-derived cell line, FLC4, using RFB culture in two experiments: inoculation of cells with infectious plasma from an HCV carrier and transfection of cells with viral RNA transcribed from the full-length cDNA of genotype 1a, which is known to infect chimpanzees. These findings prompted us to use the RFB system to create a culture model of HCV production based on genome-length dicistronic viral RNA, which has not been found to produce viral particles in standard monolayer cultures. As expected, HCV-LPs were produced and secreted into the medium during RFB culture of RCYM1 cells, whereas virus production was not observed in the conventional monolayer culture of RCYM1 cells. The presence of the viral envelope protein(s) on the HCV-LPs obtained in the RFB culture was strongly suggested from their density analysis with and without NP40 treatment.

We also created another 3D environment supportive of RCYM1 culture using TGP, a chemically synthesized biocompatible polymer which has a sol-gel transition temperature, thus enabling us to culture cells three-dimensionally in the gel phase at 37 °C and to harvest them in the sol phase at 4 °C, without enzyme digestion (Yoshioka et al., 1994). In contrast to other matrix gels made from conventional natural polymers and developed for 3D culture, including matrigel (Kleinman et al., 1986), collagen gel (Lawler et al., 1983), and soft agar, TGP has several advantages that allow us to investigate the functional characteristics of epithelial cells, their tissue-like morphology, and their potential clinical applications. The use of 3D culture materials other than TGP requires treatment with appropriate digestive enzymes or heating to collect cells grown as spheroids from the culture media, and the matrices may damage the cultured cells to some extent. Thus, it is difficult to keep the viable cells in a functionally and structurally intact. In addition, because matrigel and collagen gel are made from animal or tumor tissue, the possibility that certain pathogens or unidentified factors might influence cell function cannot be excluded. In the present study, we found that Huh-7 and RCYM1 cells formed an organized structure of spheroids after 7–10 days of culture in TGP, and that HCV-LPs were assembled and released from RCYM1 spheroids, as observed in RFB culture. It can be ruled out that HCV-LPs, RNA, and core protein detected in the TGP culture supernatant are released by damaged and/or broken cells because neither digestive enzymes nor heating is used in the culture procedures and no cell damage has been observed in the cultures.

It remains to be clarified why HCV particles were produced from Huh-7 cells harboring the genome-length dicistronic HCV RNA more efficiently in the 3D cultures than in the monolayer cultures. However, this might be related to the fact that directional protein transport in hepatocytes occurs more readily in 3D culture. EM examination demonstrated that, in the RFB and TGP culture systems, human hepatoma cells, such as Huh-7, FLC4, and FLC5 cells, self-assemble into spheroids with possible polarized morphology in which microvilli develop on the cell surface and channels resembling bile canaliculi and junction structures are created in the intercellular spaces (Aizaki et al., 2003; Iwahori et al., 2003). In contrast, human hepatoma cells adhere when grown on a plastic surface, growing as a flat monolayer without exhibiting the characteristics of polarized epithelium. In general, the interaction of viruses with polarized epithelia in the host is one of the key steps in the viral life cycle. A variety of viruses, especially enveloped viruses, mature and bud from distinct membrane domains of the host cells (Compans, 1995; Garoff et al., 1998; Schmitt and Lamb, 2004; Takimoto and Portner, 2004). For example, several respiratory viruses, such as influenza virus, parainfluenza virus, rhinovirus, and respiratory syncytial virus, are released preferentially from the apical surface. Conversely, other viruses egress from the basolateral membrane; these include vesicular stomatitis virus, Semliki Forest virus, vaccinia virus, and certain retroviruses. Thus, it is likely that more organized intracellular trafficking pathways exist in the 3D culture of Huh-7-derived cells, thereby driving the assembly and release of HCV.

The efficient production of HCV in 3D cultures could also be due to the reduction of HCV RNA replication and/or translation in 3D cultures as compared to those in monolayer cultures. RNA replication and/or translation of HCV replicons in Huh-7 cells are highly dependent on host cell growth (Pietschmann et al. 2001). In the present study, we found that the slow growth of spheroids resulted in reduced expression of HCV protein and

viral RNA in 3D-cultured RCYM1 cells compared to that in monolayer cultures containing similar cell numbers. The doubling time of cells grown in TGP or RFB culture was approximately twice that observed in monolayer culture. Although it is possible that amino acid substitutions of culture-adaptive mutations contribute to interference with virus production, another possibility might be that in cases of certain HCV clones, higher expression of the viral proteins leads to their misfolding, thereby precluding the formation of virus particles.

Complete cell culture systems for HCV have recently been developed (Lindenbach et al., 2005; Wakita et al., 2005; Zhong et al., 2005) using a genotype 2a isolate, JFH-1, obtained from a Japanese patient with fulminant hepatitis (Date et al., 2004; Kato et al., 2001, 2003). Unlike many other HCV isolates, JFH-1-based subgenomic replicons do not require culture-adaptive mutations for efficient RNA replication (Kato et al., 2003). Transfection of Huh-7 cells with the full-length JFH-1 genome or a chimeric genome using JFH-1 and J6 results in the efficient production of infectious HCV (Lindenbach et al., 2005; Wakita et al., 2005; Zhong et al., 2005). This newly established HCV culture system is undoubtedly useful for a variety of HCV studies; however, these systems rely on the JFH-1 replicase (NS3 to 5B) and little is known about the reasons that this particular isolate permits efficient HCV production. Virus yield in the 3D systems presented here is significantly lower than that in systems based on JFH-1; it seems that 0.1–1 copies of HCV RNA/cell/day are generated and assembled into viral particles. The ratio of viral RNA to the core protein in these fractions is approximately 10^5 RNA copies/1 fmol of the core. Although only moderate production of HCV particles is observed in 3D culture of RCYM1 cells, this is the first study to demonstrate the production of infectious HCV particles derived from genotype 1b, which is highly prevalent worldwide and is thought to present a higher risk of developing hepatocellular carcinoma and/or cirrhosis than infections with other HCV types (Bruno et al., 1997; Silini et al., 1996). The findings of the present study may also suggest that an extremely high efficiency of viral replication, such as that observed in the case of JFH-1 isolate, is not needed to produce HCV particles in 3D cultures of Huh-7 cells. Heller et al. (2005) report HCV virion production in a culture transfected with the genomic cDNA of genotype 1b; however, the infectivity of the virus particles remains to be determined. More recently, it was shown that chimeric HCV containing structural proteins of genotypes 1a, 1b, or 3a was produced from fusion of the core to the p7 or NS2 region with downstream nonstructural regions of JFH1 clone, but that intergenotypic chimeras frequently yielded lower titers of infectious HCV compared to JFH1 or J6/JFH1 chimera (Pietschmann et al., personal communication). The 3D culture system described in the present study might be a helpful method of increasing the efficiency of assembly and release of intergenotypic chimeric HCV.

In summary, we found that the expression of dicistronic genome-length Con1 HCV RNA of genotype 1b in 3D-cultured Huh-7 cells yields infectious virus particles, and we demonstrated the usefulness for producing HCV particles of two 3D culture systems based on RFB and TGP, in which human hepatoma cells can assemble into spheroids with potentially polarized morphology. HCV morphogenesis occurs in a complex cellular environment in which host factors may either enhance or reduce the assembly and budding process. The culture system described here will allow us to further study viral morphogenesis and the biophysical properties of HCV particles, and it provides a new tool for the future development of anti-HCV drugs.

Materials and methods

Cell lines bearing dicistronic HCV RNAs

To generate a stable cell line harboring genome-length dicistronic HCV RNA, we electroporated 10^7 Huh-7 cells with 50 μg of the RNA transcribed from a plasmid pFKI389neo/core-3′/NK5.1 (Pietschmann et al., 2002). The cells were maintained in Dulbecco's modified Eagle's medium with 10% fetal bovine serum and 0.5 mg/ml G418 (Promega). After stringent selection for 3 weeks, a fast-growing clone was isolated and designated as RCYM1. A Huh-7-derived cell line, 5–15, harboring a subgenomic replicon (Lohmann et al., 1999) was also used.

3D cell cultures

The RFB system (Able, Japan) was manipulated as described previously (Aizaki et al., 2003) with minor modifications. Briefly, the RFB column, being filled with 4 ml of porous carrier beads made from polyvinyl alcohol, seeded with 1×10^7 of RCYM1 or 5–15 cells. The cells were cultured in ASF104 medium (Ajinomoto, Japan) supplemented with 4 g/l of D-glucose, 2% fetal calf serum, and 0.5 mg/ml of G418 (Promega). TGP (Mebiol Gel MB-10; Mebiol, Japan) was supplied as a lyophilized form and its aqueous solution was prepared before use as previously described (Hishikawa et al., 2004; Nagaya et al., 2004; Yoshioka et al., 1994). Briefly, TGP in a flask was dissolved in 10 ml of the culture medium and was maintained at 4 °C overnight. To prepare HCV particles, we suspended 5×10^6 cells of RCYM1 in 10 ml of TGP solution and aliquots were poured into a multi-well plate. Upon warming to 37 °C, the TGP solution quickly turned into a gel form, and 3 volumes of the culture medium were added to cover the gel. To recover spheroid cells and the culture supernatant after cultivation, we subjected the cultured plate to a temperature of 4 °C for 10 min to dissolve the gel. In order to separate spheroid cells from the culture medium, we subsequently centrifuged the TGP culture diluted with the overlaid culture medium at 1000×*g* for 5 min.

Sucrose density gradient centrifugation

The culture medium collected from the RFB or TGP was centrifuged at 8000 × *g* for 50 min to remove all cellular debris, after which the supernatant was centrifuged at 25,000 rpm at 4 °C for 4 h with an SW28 rotor (Beckman). The precipitant was suspended in 1 ml of TNE buffer [10 mM Tris–HCl (pH 7.8), 1 mM EDTA, 100 mM NaCl] and was then layered on top of continuous 10–60% (wt/vol) sucrose gradient in TNE buffer,

followed by centrifugation at 35,000 rpm at 4 °C for 14 h with an SW41E rotor (Beckman). Fractions (1 ml each) were collected from the top of the tube (12 fractions in total). The density of each fraction was determined by the weight of 100 μl of the fraction. For NP40 treatment, 0.5 ml of the TNE-suspended sample as described above was supplemented with 10 μl of RNase inhibitor (Takara, Japan) and 5 μl of 1M DTT, which was diluted by adding NP40 solution to a final concentration of 0.2%. After incubation at 4 °C for 20 min, the sample was fractionated by discontinuous 10–60% sucrose gradient centrifugation.

Quantitation of HCV RNA and core protein

Total RNA was extracted from cells and from the culture medium using TRIZOL (Invitrogen) and a QIAamp Viral RNA Mini spin column (Qiagen), respectively. Real-time RT-PCR was performed using TaqMan EZ RT-PCR Core Reagents (PE Applied Biosystems), as described previously (Aizaki et al., 2004; Suzuki et al., 2005). HCV core antigen within cells and culture medium was measured by immunoassay (Ortho HCV-Core ELISA Kit; Ortho-Clinical Diagnotics), following the manufacturer's instructions.

Western blot analysis

The protein concentration of cells recovered from monolayer or 3D cultures was determined by BCA Protein Assay Kit (Pierce). Aliquots of samples were analyzed by sodium dodecyl sulfate–polyacrylamide gel electrophoresis (SDS–PAGE) and transferred to polyvinylidene difluoride membranes (Immobilon; Millipore, Japan) using a semidry blotter. After overnight incubation at 4 °C in blocking buffer (Dainippon Pharmaceuticals, Japan) with 0.2% Tween 20, the membranes were incubated with appropriately diluted anti-HCV core (Anogen) and anti-NS5A (Austral Biologicals) monoclonal antibody, followed by incubation with horseradish peroxidase conjugated anti-mouse immunoglobulin G (Cell Signaling). The blots were then washed and developed with enhanced SuperSignal West Pico Chemiluminecent Substrate (Pierce).

Immunocytochemistry

For NS5A staining, infected cells cultured on collagen-coated coverslips were washed with phosphate buffered saline (PBS) and fixed with 4% paraformaldehyde at 4 °C for 30 min, followed by permeabilization with PBS containing 0.2% TritonX-100. After preincubation with BlockAce (Dainippon Pharmaceuticals), the samples were stained using mouse anti-NS5A antibody and rhodamine-conjugated goat anti-mouse IgG (ICN Pharmaceuticals) as the first and second antibodies, respectively.

Electron microscopy

To visualize HCV-LPs secreted into the medium, we concentrated and adsorbed sucrose density fractions prepared as described above onto carbon-coated grids for 1 min. The grids were stained with 1% uranyl acetate for 1 min and examined under a Hitachi H-7600 transmission electron microscope. To prepare thin sections of HCV-LPs, we prefixed precipitated HCV-LPs in 2% glutaraldehyde–0.1 M cacodylate buffer at 4 °C overnight, followed by three rounds of washing with 0.1 M cacodylate buffer. The samples were then postfixed in 2% osmium tetroxide at 4 °C for 2 h, dehydrated in a graded series of ethanol solutions followed by propylene oxide, and embedded in a mixture of EPON 812, dodecenyl succinic anhydride (DDSA), methyl nadic anhydrate (MNA), and 2,4,6-tri (dimethylaminomethyl) phenol (DMP-30) at 60 °C for 2 days. Thin sections (80 nm) were stained with uranyl acetate and lead citrate. For electron microscopy of RCYM1 cells cultured in TGP, the cells were prefixed in 2% glutaraldehyde–0.1 M cacodylate buffer at 4 °C for 1 h and washed three times with 0.1 M cacodylate buffer, followed by postfixation in 2% osmium tetroxide for 3 h. After dehydration in a graded series of ethanol solutions and propylene oxide, the cells were embedded in a mixture of Epoxy 812, DDSA, MNA, and DMP-30 at 60 °C for 2 days. Thin sections (60–80 nm) were stained with 2% uranyl acetate.

Immunoelectron microscopy

HCV-LP samples were adsorbed on formvar-carbon grids and then floated for 30 min on a drop of BlockAce. Diluted anti-E2 mouse antibody was then applied for 1 h. After three rounds of washing, diluted anti-mouse IgG conjugated with 5-nm gold particles was applied for 1 h, and the grids were then stained with 1% uranyl acetate. In order to perform immunoelectron microscopy of TGP cultures using silver-intensified immunogold labeling, we fixed the cells in 4% paraformaldehyde–0.1% glutaraldehyde with 0.15 M HEPES buffer at 4 °C, followed by incubation with either anti-core rabbit antibody or anti-E1 mouse antibody overnight. After several washings, anti-rabbit or anti-mouse secondary antibody coupled with 1.4-nm-diameter gold particles (Nanoprobes) was applied overnight. The samples were then washed and fixed in 2% glutaraldehyde in 0.1 M sodium cacodylate buffer (pH 7.4) for 3 h, followed by enlargement of the gold particles with an HQ-Silver Enhancement Kit (Nanoprobes). For double staining with anti-E1 and anti-core antibodies, the cells were fixed in 7% paraformaldehyde–0.25 M sucrose in 0.03% picric acid–0.05 M cacodylate buffer at pH 7.4. Ten-nanometer gold particle-coupled anti-rabbit and 5-nm gold particle-coupled anti-mouse antibodies were used as secondary antibodies.

Assays for the infectivity of HCV-LPs and neutralization of the infection

Cell supernatant from 3D-cultured RCYM1 cells was centrifuged at 8000 × *g* for 50 min to remove all cellular debris, after which the supernatant was centrifuged at 25,000 rpm at 4 °C for 4 h with an SW28 rotor. The precipitant was suspended in 0.2–0.5 ml of ASF104 medium and the aliquot containing approximately 1×10^5 HCV RNA copies was used as each inoculum. Huh-7.5.1

cells (provided by Dr. F. V. Chisari, The Scripps Research Institute) (Zhong et al., 2005), which were seeded at a density of 10^4 cells/well in a 48-well plate 24 h before infection. The inocula were incubated for 3 h, followed by 3 rounds of washing with PBS and the addition of complete medium. For the kinetics assay, cells were harvested 0, 1, 2, 3, and 7 days after infection and the amount of intracellular HCV RNA was quantified as described above. Infection with HCV-LP was determined after 4 days by immunofluorescence staining for HCV NS5A. In the neutralization assay, the HCV-LP samples were incubated with the anti-E2 antibody AP33 (Owsianka et al., 2005) at 10 μg/ml (kindly provided by Dr. A. H. Patel, University of Glasgow, UK), with the human sera with high titers of NOB antibodies NOB3 and NOB4 (Ishii et al., 1998), or with anti-FLAG antibody (Sigma) at 10 μg/ml for 1 h at 37 °C prior to infection. Anti-human CD81 antibody (BD Pharmigen) at 10 μg/ml was preincubated with Huh-7.5.1 cells for 1 h at 37 °C, followed by being washed with PBS three times. HCV-LP derived from TGP-cultured RCYM1 cells or JFH1 virus was incubated with these cells, as mentioned above. JFH1 virus was prepared from pJFH1 (Wakita et al., 2005), which contains the full-length cDNA of JFH1 isolate and was kindly provided by T. Wakita (Tokyo Metropolitan Institute for Neuroscience, Japan), as described (Wakita et al., 2005). The cells were harvested 4 days after infection and neutralizing activity was assessed by quantifying the amount of intracellular HCV RNA as described above.

Assay for anti-HCV-LP production

At the initiation of the 3D culture of RCYM1 cells (5×10^5 in 1 ml TGP), 100 IU/ml IFN-α (Sumiferon 300; Sumitomo Pharmaceuticals, Japan), or 100 μM RBV (MP Biomedicals, Germany) were added and the cells were cultured for 5 days. Culture media were harvested and fractionated by sucrose density centrifugation as described above. Total RNAs were extracted from aliquots of 1.18 g/ml (HCV-LP positive) and 1.04 g/ml (HCV-LP-negative) fractions, followed by quantification of viral RNA.

Acknowledgments

The authors would like to thank Francis V. Chisari of The Scripps Research Institute, Arvind H. Patel of the University of Glasgow, and Takaji Wakita of Tokyo Metropolitan Institute for Neuroscience for providing Huh-7.5.1 cells, anti-E2 antibody, and pJFH1, respectively. We also thank Mami Matsuda, Tetsu Shimoji, and Makiko Yahata for technical assistance, and Tomoko Mizoguchi for her secretarial work. This work was supported in part by a grant for Research on Health Sciences focusing on Drug Innovation from the Japan Health Sciences Foundation; by grants-in-aid from the Ministry of Health, Labor and Welfare; by a Sasagawa Scientific Research Grant from the Japan Science Society; and by the program for Promotion of Fundamental Studies in Health Sciences of the National Institute of Biomedical Innovation (NBIO), Japan; and by the New Energy and Industrial Technology Development Organization (NEDO) of Japan.

References

Aizaki, H., Nagamori, S., Matsuda, M., Kawakami, H., Hashimoto, O., Ishiko, H., Kawada, M., Matsuura, T., Hasumura, S., Matsuura, Y., Suzuki, T., Miyamura, T., 2003. Production and release of infectious hepatitis C virus from human liver cell cultures in the three-dimensional radial-flow bioreactor. Virology 314, 16–25.

Aizaki, H., Lee, K.J., Sung, V.M., Ishiko, H., Lai, M.M., 2004. Characterization of the hepatitis C virus RNA replication complex associated with lipid rafts. Virology 324, 450–461.

Andre, P., Komurian-Pradel, F., Deforges, S., Perret, M., Berland, J.L., Sodoyer, M., Pol, S., Brechot, C., Paranhos-Baccala, G., Lotteau, V., 2002. Characterization of low- and very-low-density hepatitis C virus RNA-containing particles. J. Virol. 76, 6919–6928.

Bartosch, B., Cosset, F.L., 2006. Cell entry of hepatitis C virus. Virology (Electronic publication ahead of print).

Baumert, T.F., Ito, S., Wong, D.T., Liang, T.J., 1998. Hepatitis C virus structural proteins assemble into viruslike particles in insect cells. J. Virol. 72, 3827–3836.

Blanchard, E., Brand, D., Trassard, S., Goudeau, A., Roingeard, P., 2002. Hepatitis C virus-like particle morphogenesis. J. Virol. 76, 4073–4079.

Blanchard, E., Hourioux, C., Brand, D., Ait-Goughoulte, M., Moreau, A., Trassard, S., Sizaret, P.Y., Dubois, F., Roingeard, P., 2003. Hepatitis C virus-like particle budding: role of the core protein and importance of its Asp111. J. Virol. 77, 10131–10138.

Blight, K.J., Kolykhalov, A.A., Rice, C.M., 2000. Efficient initiation of HCV RNA replication in cell culture. Science 290, 1972–1974.

Blight, K.J., McKeating, J.A., Rice, C.M., 2002. Highly permissive cell lines for subgenomic and genomic hepatitis C virus RNA replication. J. Virol. 76, 13001–13014.

Bruno, S., Silini, E., Crosignani, A., Borzio, F., Leandro, G., Bono, F., Asti, M., Rossi, S., Larghi, A., Cerino, A., Podda, M., Mondelli, M.U., 1997. Hepatitis C virus genotypes and risk of hepatocellular carcinoma in cirrhosis: a prospective study. Hepatology 25, 754–758.

Choo, Q.L., Kuo, G., Weiner, A.J., Overby, L.R., Bradley, D.W., Houghton, M., 1989. Isolation of a cDNA clone derived from a blood-borne non-A, non-B viral hepatitis genome. Science 244, 359–362.

Choo, Q.L., Richman, K.H., Han, J.H., Berger, K., Lee, C., Dong, C., Gallegos, C., Coit, D., Medina-Selby, R., Barr, P.J., et al., 1991. Genetic organization and diversity of the hepatitis C virus. Proc. Natl. Acad. Sci. U.S.A. 88, 2451–2455.

Compans, R.W., 1995. Virus entry and release in polarized epithelial cells. Curr. Top. Microbiol. Immunol. 202, 209–219.

Date, T., Kato, T., Miyamoto, M., Zhao, Z., Yasui, K., Mizokami, M., Wakita, T., 2004. Genotype 2a hepatitis C virus subgenomic replicon can replicate in HepG2 and IMY-N9 cells. J. Biol. Chem. 279, 22371–22376.

Davis, G.L., Wong, J.B., McHutchison, J.G., Manns, M.P., Harvey, J., Albrecht, J., 2003. Early virologic response to treatment with peginterferon alfa-2b plus ribavirin in patients with chronic hepatitis C. Hepatology 38, 645–652.

Frese, M., Pietschmann, T., Moradpour, D., Haller, O., Bartenschlager, R., 2001. Interferon-alpha inhibits hepatitis C virus subgenomic RNA replication by an MxA-independent pathway. J. Gen. Virol. 82, 723–733.

Garoff, H., Hewson, R., Opstelten, D.J., 1998. Virus maturation by budding. Microbiol. Mol. Biol. Rev. 62, 1171–1190.

Grakoui, A., McCourt, D.W., Wychowski, C., Feinstone, S.M., Rice, C.M., 1993. Characterization of the hepatitis C virus-encoded serine proteinase: determination of proteinase-dependent polyprotein cleavage sites. J. Virol. 67, 2832–2843.

Guo, J.T., Bichko, V.V., Seeger, C., 2001. Effect of alpha interferon on the hepatitis C virus replicon. J. Virol. 75, 8516–8523.

Heller, T., Saito, S., Auerbach, J., Williams, T., Moreen, T.R., Jazwinski, A., Cruz, B., Jeurkar, N., Sapp, R., Luo, G., Liang, T.J., 2005. An in vitro model of hepatitis C virion production. Proc. Natl. Acad. Sci. U.S.A. 102, 2579–2583.

Hijikata, M., Kato, N., Ootsuyama, Y., Nakagawa, M., Shimotohno, K., 1991. Gene mapping of the putative structural region of the hepatitis C virus genome by in vitro processing analysis. Proc. Natl. Acad. Sci. U.S.A. 88, 5547–5551

Hishikawa, K., Miura, S., Marumo, T., Yoshioka, H., Mori, Y., Takato, T., Fujita, T., 2004. Gene expression profile of human mesenchymal stem cells during osteogenesis in three-dimensional thermoreversible gelation polymer. Biochem. Biophys. Res. Commun. 317, 1103–1107.

Ikeda, M., Yi, M., Li, K., Lemon, S.M., 2002. Selectable subgenomic and genome-length dicistronic RNAs derived from an infectious molecular clone of the HCV-N strain of hepatitis C virus replicate efficiently in cultured Huh7 cells. J. Virol. 76, 2997–3006.

Ishii, K., Rosa, D., Watanabe, Y., Katayama, T., Harada, H., Wyatt, C., Kiyosawa, K., Aizaki, H., Matsuura, Y., Houghton, M., Abrignani, S., Miyamura, T., 1998. High titers of antibodies inhibiting the binding of envelope to human cells correlate with natural resolution of chronic hepatitis C. Hepatology 28, 1117–1120.

Iwahori, T., Matsuura, T., Maehashi, H., Sugo, K., Saito, M., Hosokawa, M., Chiba, K., Masaki, T., Aizaki, H., Ohkawa, K., Suzuki, T., 2003. CYP3A4 inducible model for in vitro analysis of human drug metabolism using a bioartificial liver. Hepatology 37, 665–673.

Kanto, T., Hayashi, N., Takehara, T., Hagiwara, H., Mita, E., Naito, M., Kasahara, A., Fusamoto, H., Kamada, T., 1994. Buoyant density of hepatitis C virus recovered from infected hosts: two different features in sucrose equilibrium density-gradient centrifugation related to degree of liver inflammation. Hepatology 19, 296–302.

Kato, T., Furusaka, A., Miyamoto, M., Date, T., Yasui, K., Hiramoto, J., Nagayama, K., Tanaka, T., Wakita, T., 2001. Sequence analysis of hepatitis C virus isolated from a fulminant hepatitis patient. J. Med. Virol. 64, 334–339.

Kato, T., Date, T., Miyamoto, M., Furusaka, A., Tokushige, K., Mizokami, M., Wakita, T., 2003. Efficient replication of the genotype 2a hepatitis C virus subgenomic replicon. Gastroenterology 125, 1808–1817.

Kawada, M., Nagamori, S., Aizaki, H., Fukaya, K., Niiya, M., Matsuura, T., Sujino, H., Hasumura, S., Yashida, H., Mizutani, S., Ikenaga, H., 1998. Massive culture of human liver cancer cells in a newly developed radial flow bioreactor system: ultrafine structure of functionally enhanced hepatocarcinoma cell lines. In Vitro Cell. Dev. Biol. Anim. 34, 109–115.

Kleinman, H.K., McGarvey, M.L., Hassell, J.R., Star, V.L., Cannon, F.B., Laurie, G.W., Martin, G.R., 1986. Basement membrane complexes with biological activity. Biochemistry 25, 312–318.

Lawler, E.M., Miller, F.R., Heppner, G.H., 1983. Significance of three-dimensional growth patterns of mammary tissues in collagen gels. In Vitro 19, 600–610.

Lindenbach, B.D., Evans, M.J., Syder, A.J., Wolk, B., Tellinghuisen, T.L., Liu, C.C., Maruyama, T., Hynes, R.O., Burton, D.R., McKeating, J.A., Rice, C.M., 2005. Complete replication of hepatitis C virus in cell culture. Science 309, 623–626.

Lohmann, V., Korner, F., Koch, J., Herian, U., Theilmann, L., Bartenschlager, R., 1999. Replication of subgenomic hepatitis C virus RNAs in a hepatoma cell line. Science 285, 110–113.

Manns, M.P., McHutchison, J.G., Gordon, S.C., Rustgi, V.K., Shiffman, M., Reindollar, R., Goodman, Z.D., Koury, K., Ling, M., Albrecht, J.K., 2001. Peginterferon alfa-2b plus ribavirin compared with interferon alfa-2b plus ribavirin for initial treatment of chronic hepatitis C: a randomised trial. Lancet 358, 958–965.

Matsuura, T., Kawada, M., Hasumura, S., Nagamori, S., Obata, T., Yamaguchi, M., Hataba, Y., Tanaka, H., Shimizu, H., Unemura, Y., Nonaka, K., Iwaki, T., Kojima, S., Aizaki, H., Mizutani, S., Ikenaga, H., 1998. High density culture of immortalized liver endothelial cells in the radial-flow bioreactor in the development of an artificial liver. Int. J. Artif. Organs 21, 229–234.

Nagaya, M., Kubota, S., Suzuki, N., Tadokoro, M., Akashi, K., 2004. Evaluation of thermoreversible gelation polymer for regeneration of focal liver injury. Eur. Surg. Res. 36, 95–103.

Nakajima, N., Hijikata, M., Yoshikura, H., Shimizu, Y.K., 1996. Characterization of long-term cultures of hepatitis C virus. J. Virol. 70, 3325–3329.

Netski, D.M., Mosbruger, T., Depla, E., Maertens, G., Ray, S.C., Hamilton, R.G., Roundtree, S., Thomas, D.L., McKeating, J., Cox, A., 2005. Humoral immune response in acute hepatitis C virus infection. Clin. Infect. Dis. 41, 667–675.

Owsianka, A., Tarr, A.W., Juttla, V.S., Lavillette, D., Bartosch, B., Cosset, F.L., Ball, J.K., Patel, A.H., 2005. Monoclonal antibody AP33 defines a broadly neutralizing epitope on the hepatitis C virus E2 envelope glycoprotein. J. Virol. 79, 11095–11104.

Pietschmann, T., Lohmann, V., Rutter, G., Kurpanek, K., Bartenschlager, R., 2001. Characterization of cell lines carrying self-replicating hepatitis C virus RNAs. J. Virol. 75, 1252–1264.

Pietschmann, T., Lohmann, V., Kaul, A., Krieger, N., Rinck, G., Rutter, G., Strand, D., Bartenschlager, R., 2002. Persistent and transient replication of full-length hepatitis C virus genomes in cell culture. J. Virol. 76, 4008–4021.

Pileri, P., Uematsu, Y., Campagnoli, S., Galli, G., Falugi, F., Petracca, R., Weiner, A.J., Houghton, M., Rosa, D., Grandi, G., Abrignani, S., 1998. Binding of hepatitis C virus to CD81. Science 282, 938–941.

Rosa, D., Campagnoli, S., Moretto, C., Guenzi, E., Cousens, L., Chin, M., Dong, C., Weiner, A.J., Lau, J.Y., Choo, Q.L., Chien, D., Pileri, P., Houghton, M., Abrignani, S., 1996. A quantitative test to estimate neutralizing antibodies to the hepatitis C virus: cytofluorimetric assessment of envelope glycoprotein 2 binding to target cells. Proc. Natl. Acad. Sci. U.S.A. 93, 1759–1763.

Sasaki, M., Yamauchi, K., Nakanishi, T., Kamogawa, Y., Hayashi, N., 2003. In vitro binding of hepatitis C virus to CD81-positive and -negative human cell lines. J. Gastroenterol. Hepatol. 18, 74–79.

Schmitt, A.P., Lamb, R.A., 2004. Escaping from the cell: assembly and budding of negative-strand RNA viruses. Curr. Top. Microbiol. Immunol. 283, 145–196.

Shimizu, Y.K., Feinstone, S.M., Kohara, M., Purcell, R.H., Yoshikura, H., 1996. Hepatitis C virus: detection of intracellular virus particles by electron microscopy. Hepatology 23, 205–209.

Silini, E., Bottelli, R., Asti, M., Bruno, S., Candusso, M.E., Brambilla, S., Bono, F., Iamoni, G., Tinelli, C., Mondelli, M.U., Ideo, G., 1996. Hepatitis C virus genotypes and risk of hepatocellular carcinoma in cirrhosis: a case–control study. Gastroenterology 111, 199–205.

Suzuki, T., Omata, K., Satoh, T., Miyasaka, T., Arai, C., Maeda, M., Matsuno, T., Miyamura, T., 2005. Quantitative detection of hepatitis C virus (HCV) RNA in saliva and gingival crevicular fluid of HCV-infected patients. J. Clin. Microbiol. 43, 4413–4417.

Takimoto, T., Portner, A., 2004. Molecular mechanism of paramyxovirus budding. Virus Res. 106, 133–145.

Trestard, A., Bacq, Y., Buzelay, L., Dubois, F., Barin, F., Goudeau, A., Roingeard, P., 1998. Ultrastructural and physicochemical characterization of the hepatitis C virus recovered from the serum of an agammaglobulinemic patient. Arch. Virol. 143, 2241–2245.

Wakita, T., Pietschmann, T., Kato, T., Date, T., Miyamoto, M., Zhao, Z., Murthy, K., Habermann, A., Krausslich, H.G., Mizokami, M., Bartenschlager, R., Liang, T.J., 2005. Production of infectious hepatitis C virus in tissue culture from a cloned viral genome. Nat. Med. 11, 791–796.

Yi, M.K., Villanueva, R.A., Thomas, D., Wakita, T., Lemon, S.M., 2006. Production of infectious genotype 1a hepatitis C virus (Hutchinson strain) in cultured human hepatoma cells. Proc. Natl. Acad. Sci. U.S.A. 103, 2310–2315.

Yoshioka, H., Mikami, M., Mori, Y., Tsuchida, E., 1994. A synthetic hydrogel with thermoreversible gelation. J. Macromol. Sci. A31, 113–120.

Zhong, J., Gastaminza, P., Cheng, G., Kapadia, S., Kato, T., Burton, D.R., Wieland, S.F., Uprichard, S.L., Wakita, T., Chisari, F.V., 2005. Robust hepatitis C virus infection in vitro. Proc. Natl. Acad. Sci. U.S.A. 102, 9294–9299.

J. Biochem. 139, 921–930 (2006)
doi:10.1093/jb/mvj104

Proteomic Profiling of Lipid Droplet Proteins in Hepatoma Cell Lines Expressing Hepatitis C Virus Core Protein

Shigeko Sato[1], Masayoshi Fukasawa[1,*], Yoshio Yamakawa[1], Tohru Natsume[2], Tetsuro Suzuki[3], Ikuo Shoji[3], Hideki Aizaki[3], Tatsuo Miyamura[3] and Masahiro Nishijima[1,†]

[1]Department of Biochemistry and Cell Biology and [3]Department of Virology II, National Institute of Infectious Diseases, Tokyo 162-8640; and [2]National Institute of Advanced Industrial Science and Technology (AIST), Biological Information Research Center, Tokyo 135-0064

Received February 7, 2006; accepted April 4, 2006

Hepatitis C virus (HCV) core protein has been suggested to play crucial roles in the pathogeneses of liver steatosis and hepatocellular carcinomas due to HCV infection. Intracellular HCV core protein is localized mainly in lipid droplets, in which the core protein should exert its significant biological/pathological functions. In this study, we performed comparative proteomic analysis of lipid droplet proteins in core-expressing and non-expressing hepatoma cell lines. We identified 38 proteins in the lipid droplet fraction of core-expressing (Hep39) cells and 30 proteins in that of non-expressing (Hepswx) cells by 1-D-SDS-PAGE/MALDI-TOF mass spectrometry (MS) or direct nanoflow liquid chromatography–MS/MS. Interestingly, the lipid droplet fraction of Hep39 cells had an apparently lower content of adipose differentiation-related protein and a much higher content of TIP47 than that of Hepswx cells, suggesting the participation of the core protein in lipid droplet biogenesis in HCV-infected cells. Another distinct feature is that proteins involved in RNA metabolism, particularly DEAD box protein 1 and DEAD box protein 3, were detected in the lipid droplet fraction of Hep39 cells. These results suggest that lipid droplets containing HCV core protein may participate in the RNA metabolism of the host and/or HCV, affecting the pathopoiesis and/or virus replication/production in HCV-infected cells.

Key words: ADRP, DEAD box protein, hepatitis C virus, lipid droplet, TIP47.

Abbreviations: HCV, hepatitis C virus; HCC, hepatocellular carcinoma; MS, mass spectrometry; DNLC, direct nanoflow liquid chromatography; HRP, horseradish peroxidase; ADRP, adipose differentiation-related protein; DDX1, DEAD box protein 1; DDX3, DEAD box protein 3.

Hepatitis C virus (HCV) is a major causative agent of chronic hepatitis (*1*, *2*). Persistent HCV infection, which occurs in more than 70% of infected patients, is strongly associated with the development of liver steatosis, which involves the accumulation of intracellular lipid droplets, cirrhosis, and hepatocellular carcinomas (HCC) (*3*, *4*). Since more than 170 million people in the world are currently infected with HCV (*1*), and there is no cure that is completely effective, understanding the mechanism by which HCV induces serious liver diseases is one of the most important global public health issues. HCV, a member of the *Flaviviridae* family, possesses a single-stranded, positive-sense RNA genome of ~9.6 kb (*5*). The HCV genome has a single open reading frame that codes for a large precursor polyprotein of ~3,000 amino acids that is processed into at least 10 individual proteins by host and viral proteases (*6*).

HCV core protein, the product of the N-terminal portion of the polyprotein, generated upon cleavage at the endoplasmic reticulum by signal peptidase and signal peptide peptidase (*7*, *8*), forms the nucleocapsid of an HCV virion (*9*). Interestingly, in addition to its function as a structural protein, the core protein exhibits activities leading host cells to lipogenic and malignant transformation *in vitro* (*10–12*). Moreover, transgenic mice expressing HCV core protein developed liver steatosis and HCC (*13*, *14*), suggesting an important role of the core protein in these diseases. Many studies have shown that HCV core protein substantially affects various cellular regulatory processes, such as gene transcription (*15–17*) and signal transduction pathways (*12*, *18–23*), and interacts with a variety of host proteins (*12*, *18*, *19*, *22*, *24–34*), but it is not clear what activities/molecules are practically relevant to the pathogeneses of HCV (core)-derived liver steatosis and HCC. Extensive screenings for genes/proteins exhibiting differences in cellular expression by cDNA microarray (*35–40*) or proteome analysis (*41*, *42*) have also been tried for HCV-related HCC. Although various genes/proteins were identified, further studies are required to identify the molecules eventually involved in the pathogenesis of HCV-related HCC.

In host cells, HCV core protein is distributed mainly in lipid droplets and the endoplasmic reticulum (*7*, *10*, *43–46*), in which the core protein is predicted to exert its significant biological/pathological functions. In this study, we thus focused on HCV core protein and lipid droplets, and

*To whom correspondence should be addressed. Tel: +81-3-5285-1111, Fax: +81-3-5285-1157, E-mail: fuka@nih.go.jp
†Present address: Department of Clinical Pharmacy, Faculty of Pharmaceutical Sciences, Doshisha Women's College of Liberal Arts, Kyoto 610-0395.

